NTNU – Trondheim
Norwegian University of
Science and Technology

Realized GARCH: Evidence in ICE Brent Crude Oil Futures Front Month Contracts

Sindre Solibakke

Master of Science in Physics and Mathematics
Submission date: June 2012
Supervisor: Arvid Næss, MATH

Norwegian University of Science and Technology
Department of Mathematical Sciences

Preface

This thesis completes my master's degree in Industrial Mathematics at the Norwegian University of Science and Technology (NTNU). The work has been carried out at the Department of Mathematical Sciences during the spring semester of 2012 under the supervision of Professor Arvid Næss.

I would like to thank Arvid Næss for guidance and help throughout the semester. I would also like to thank participants at the 2012 ElCarbon-Risk seminar at Molde University College with special thanks to Erik Haugom, Sjur Westgaard, Paul C. Kettler, Gudbrand Lien and Per Bjarte Solibakke.

Finally i would like to thank my friends and family for providing me with both moral support and distractions when needed.

Sindre Solibakke

June 12, 2012

Trondheim

Abstract

This paper extends standard GARCH models of volatility with realized measures for the realized GARCH framework. A key feature of the realized GARCH framework is the measurement equation that relates the observed realized measure to latent volatility. We pay special attention to linear and log-linear realized GARCH models. Moreover, the framework enhance the joint modeling of returns and realized measures of volatility. An empirical application with ICE Brent Crude Oil future front month contracts shows that a realized GARCH specification improves the empirical fit substantially relative to a standard GARCH model. The estimates give weak evidence for a skewed student's t distribution for the standardized error term and the leverage function shows a clear negative asymmetry between today's return and tomorrow's volatility.

Sammendrag

Denne artikkelen viderefører standard GARCH modeller for volatilitet med realiserte målinger for realized GARCH rammeverket. Et nøkkelmoment for realized GARCH rammeverket er målingsligningen som relaterer den observerte realiserte målingen til latent volatilitet. Vi legger spesielt vekt på lineære og log-lineære realized GARCH modeller. Rammeverket forbedrer felles modelleringen for avkastning og realiserte målinger av volatilitet. En empirisk studie med ICE Brent Crude Oil future front month kontrakter viser at en realized GARCH spesifikasjon forbedrer den empiriske tilpasningen mye, relativt til en standard GARCH model. Estimeringene gir svake bevis for en skjev student's t fordeling for det standardiserte feil leddet og leverage funksjonen viser en klar negativ asymmetri mellom dagens avkastning og neste dags volatilitet.

Contents

Chapter 1

Introduction

This paper incorporates high frequency data and realized volatility measures for volatility modeling using GARCH models. The access to high frequency data from oil markets, make realized GARCH applications possible. The main objective of the paper is therefore to improve volatility estimation in oil markets using high frequency data.

Volatility estimation is an important tool for a wide range of application. There has been a significant amount of research on the estimation of volatility and quite a number of models has been designed. International literature has a remarkable number of papers and applications. The literature shows that volatility models seem to capture most of the features found in financial markets.

These models are based on methods developed in the financial literature. In this paper oil future prices and the underlying volatility will be modeled based on the financial framework. (Bystrom 2005) showed that financial energy markets have much of the same features as a financial market and in some cases they are identical.

The first model that was developed in the financial literature was the ARCH model, introduced in the seminar paper from (Engle 1982). The GARCH framework, introduced by (Bollerselv 1986), applies daily or weekly asset returns to specify the latent conditional volatility. A GARCH model typically uses daily returns to say something about the present and future level of volatility. Understanding the conditional volatility is important for many applications, especially option pricing, risk management and asset allocation.

In recent years high-frequency financial data has become available for a broad range of markets. The financial data consists of tick-by-tick observations with information such as time, date and price. The use of tick-by-tick return data was first discussed in the seminar paper of (Dacorogna 2001). These results led to the suggestion that high frequency data was superior to daily returns. The next innovation was a series of papers that managed to relate high frequency data to the

quadratic variation theory (stochastic volatility). From this research came the concept commonly known as realized variation. The main ideas and motivation was first discussed in the papers of, (Andersen & Bollerslev 1998), (Barndorff-Nielsen & Shephard 2001) and (Comte & Renault 1998). These important papers suggested a nonparametric ex-post estimate of the return variation, known as realized volatility. They also show that forecasting realized volatility is a better forecasting tool then classical GARCH-X volatility forecasting.

However, more recently extended GARCH models has been constructed to incorporate realized measures. The MEM model introduced by (Engle & Gallo 2006) and the HEAVY model by (Shephard & Sheppard 2010) are two models which incorporates realized measures. The models are based on the GARCH framework and adds an additional GARCH structure for each realized measure. Models with potential several latent volatility structures can then be added. A conceptually similar model related to the realized measures are the realized GARCH model introduced by (Hansen, Huang & Shek 2011). This model is closely related to the standard GARCH model, but includes a measurement equation that relates the realized measures to latent volatility. While the MEM and HEAVY models have several latent volatility factors, the realized GARCH model only has one. The general structure of a realized GARCH(p,q) model can be represented with the following tree equations

$$\begin{aligned} r_t &= \sqrt{h_t} z_t \\ h_t &= \omega + \sum_{i=1}^{p} \beta_i h_{t-i} + \sum_{j=1}^{q} \gamma_j x_{j-i} \\ x_t &= \xi + \phi h_t + \tau(z_t) + u_t \end{aligned}$$

where r_t is the return, $z_t \sim iid(0,1)$, $u_t \sim iid(0,\sigma_u)$ and $h_t = var(r_t|F_{t1})$ with $F_t = \sigma(r_t, x_t, r_{t1}, x_{t1}, ...)$. The last equation, x_t , is known as the measurement equation. $\tau(z_t)$ represents the leverage function on the form $\tau(z_t) = \tau_1 z_t + \tau_2(z_t^2 1)$. This function estimates the correlation between daily return and future volatility which results in significant improvements for the empirical fit. The structure of the model together with a quadratic leverage function, makes the model simple to estimate. The model initially assumes a standard normal distribution for the standardized error term, z_t. However, distributions like the student's t and skewed student's t can also be included without redefining the maximum likelihood analysis.

In this paper quadratic variation theory is applied to ICE Brent Crude oil future front month contracts. Realized measure using high frequency data for the contracts will be represented and discussed. Furthermore, the realized measures will be implemented as described above, and used to estimate the realized GARCH model. The Log-likelihood will be used to compare the different models. The main results show that high frequency data, in GARCH models, improves the log-likelihood and therefore suggests improved estimation for the oil future market.

There is also found evidence for a clear asymmetry between today's return and tomorrows volatility.

The paper is organized as follows. Section 2 introduces quadratic variation theory with special emphasis on the realized measures. Section 3 introduces the realized GARCH model with a linear and log linear specification. The leverage effect and news impact curve is discussed and the quasi maximum likelihood estimator is given together with the asymptotic properties. Distributions for the standardized error term, z_t, is given together with their respective log-likelihood functions. Section 4 gives empirical results for the ICE Brent Crude oil future front month contract. The results include realized variance, jump variation, realized GARCH estimates, asymmetries and news impact curves. Section 5 summarizes and concludes.

Chapter 2

Quadratic variation theory and Realized volatility

This section will introduce quadratic variation theory (QVT). Oil future prices often follows specific characteristics including the existence of extreme jumps. Jump-diffusion models are common for identifying these kinds of jump variations in asset price dynamics, (Barndorff-Nielsen & Shephard 2004, Andersen, Bollerslev & Diebold 2007). Let $p(t)$ donate the spot price of some asset, and that this price is governed by a jump-diffusion process,

$$dp(t) = \mu(t)dt + \sigma(t)dW(t) + \kappa(t)dq(t) \tag{2.1}$$

where $\mu(t)$ and $\sigma(t)$ are the drift and instantaneous volatility, $W(t)$ is a standard Brownian motion, and $q(t)$ is a Poisson counting process, with the corresponding time-varying intensity function $\lambda(t)$. $\lambda(t)$ is the intensity of arrival process for jumps, with corresponding jump size $\kappa(t)$ for any time t given that $dq(t) = 1$.

These Jumps gives an addition to the unobserved quadratic variation. The overall variation is influenced by the number of jumps and their respective sizes. Quadratic variation theory allows us to split the total variation, non-parametrically, into a continuous simple path part and a jump part. The total quadratic variation can then be represented as,

$$QV_t = \int_0^t \sigma^2(s)ds + \sum_{s=1}^{q(t)} \kappa^2(s) \tag{2.2}$$

Eq. (2.2) implies that with absence of jumps, the sum over the squared jump sizes would be zero. Which again implies that the quadratic variation would be equal to the integrated variance,

$$IV_t = \int_0^t \sigma^2(s)ds \tag{2.3}$$

Theoretically, jump-diffusion models are intuitive, but for real data the models becomes difficult to estimate. (Andersen, Bollerslev, Diebold & Ebens 2001) proposed to use the so-called realized variation or realized volatility as a proxy for the unobserved quadratic variation represented above. They assumed that if the frequency (M) of intradaily sampling increases then the quadratic variation could be written as,

$$\lim_{M\to\infty} RV_t = \int_0^t \sigma^2(s)ds + \sum_{s=1}^{q(t)} \kappa^2(s) \tag{2.4}$$

Assume that there is high frequency data for some asset price over a period of T days. The high frequency data can then be samples at frequency (M) over a period of T days. If the data is sampled at equally spaced intervals, the intradaily returns may be represented as,

$$r_{t,j} = p_{t,j} - p_{t,j-1}, \quad j = 1, ..., M, \quad t = 1, ..., T \tag{2.5}$$

Assuming that the sample contains a relatively high frequency (M), the drift $\mu(t)$ in Eq. (2.1) is negligible. Hence, the realized variance in Eq. (2.4) can be represented as the sum of squared intradaily returns,

$$RV_t = \sum_{j=1}^{M} r_{t,j}^2 \tag{2.6}$$

This estimator is directly effected by the used sampling frequency. Eq. (2.4) shows how the RV_t estimator increases in precision when the sampling frequency increases. Theoreticaly the optimal estimator would use the lowest resulution of data avalible. In reality, the frequency used need to reflect the market features. The ICE Brent Crude future market has high liquidity in the front month contracts. Hence, the frequency of trading and the micro structure noise might directly influence the result for closely sampled observations. Lower frequency of trading and possibly a noisy bid/ask spread, would directly influence the estimators predictive abilities. The resolution of data used will be discussed in more depth later in this paper. (Barndorff-Nielsen & Shephard 2004) introduced a new extension to the realized power variation, realized bipower variation. This estimate was proved quite robust, implying that if there is stochastic volatility in connection with jumps, the realized bipower variation estimates the quadratic variation of the jump component. The realized bipower variation is defined by,

$$BVar_t = \mu_1^{-2} \sum_{j=1}^{M-1} |r_{t,j}||r_{t,j-1}|, \quad t = 1, ..., T \tag{2.7}$$

where $\mu_1 = \sqrt{\frac{2}{\pi}}$. They also showed that the realized bipower variation has the same properties as the realized variance when the resolution of data increases,

$$\lim_{M\to\infty} BVar_t \to \int_0^t \sigma^2(s)ds \tag{2.8}$$

It was first noted by (Barndorff-Nielsen & Shephard 2004) that combining Eq. (2.4) and Eq. (2.8) could give a reasonable estimate for the discontinuous jump part of the quadratic variation. Assume that there is a constant δ which has the following property, $\delta \to 0$, then the contribution to the quadratic variation process due to the discontinuities can be estimated by,

$$RV_t(\delta) - BVar_t(\delta) = \sum_{s=1}^{q(t)} \kappa^2(s) \tag{2.9}$$

Eq. (2.7) is called the first lag estimate of the bipower variation. The bipower variation becomes a good estimate if there is high evidence of jumps occurring throughout the data. The energy market is one such market where you can expect the existence of both frequent and extreme jumps. (Huang & Tauchen 2005) introduced a modification to the bipower variation, namely second lag bipower variation estimated for each day t represented as,

$$BVar_t = \frac{1}{\mu_1^2(1 - \frac{2}{M})} \sum_{j=3}^{M} |r_{t,j}||r_{t,j-2}|, \quad t = 1, ..., T \tag{2.10}$$

(Huang & Tauchen 2005) found that the second-lag bipower variation in Eq. (2.10) reduces the influence microstructure noise has on the bias for finding jumps. More specific, it reduces the local serial correlation induced by microstructure noise. Using the measure defined in Eq. (2.10), (Bollerslev, Kretschmer, Pigorsch & Tauchen 2009) found that one possible way of defining jumps could be represented as,

$$JVar_t = RVar_t - BVar_t \tag{2.11}$$

where $JVar_t$ represents the jump variation. Theoretically, the jump variation is restricted to be non-negative, but there might occur negative values for specific values of M in practice. Hence, the value of $JVar_t$ is of importance when it comes to identifying actual jumps. It is then reasonable to consider all values beyond a certain threshold to be significant jumps. (Andersen, Bollerslev & Dobrev 2007b) and (Lee & Mykland 2008) proposed a Z-test statistic for finding these significant jumps. The statistic is represented as

$$Z(t, i) = \frac{r_{t,i}}{\hat{\sigma}(t, i)}, \tag{2.12}$$

where

$$\hat{\sigma}(t, i)^2 = \frac{1}{K - 2} \sum_{j=i-K+2}^{i-1} |r_{t,i}||r_{t,i-1}| \tag{2.13}$$

The bipower variation is used as the measure for volatility in the denominator, which suggests that the method is somewhat robust. The variation is calculated over a period with K observations where K is based on the observation frequency. (Lee & Mykland 2008) proposed to use $K = 110$, 156 and 270 with respective observation frequencies 30, 15 and 5 minutes. Under the null hypothesis of no

jumps the Z-test has a normal distribution with the same properties as the z-test introduced by (Huang & Tauchen 2005). To suggest a rejection region (Lee & Mykland 2008) proposed to look at the distribution of maxima for the Z-test. They showed that when the observation frequency goes to zero the absolute value of the statistic converges to a Gumbel distribution,

$$\frac{\max_{i,j} |Z(t,j)| - C_n}{S_n} \xrightarrow{d} \zeta \tag{2.14}$$

where ζ is standard Gumbel distributed.

$$C_n = \frac{(2\log n)^{1/2}}{\mu} - \frac{\log \pi + \log(\log n)}{2\mu(2\log n)^{1/2}}, \quad \text{and} \quad S_n = \frac{1}{\mu(2\log n)^{1/2}}$$

where n is the number of intraday observations for each period t. Hence, using the Gumbel distribution, we reject the hypothesis of no jumps at time t, i when

$$\frac{|Z(t,i)| - C_n}{S_n} > \beta,$$

given that $\exp(-e^{-\beta}) = 1 - \alpha$, i.e. $\beta = -\log(-\log(1-\alpha))$, where α is the significance level.(Andersen, Bollerslev, Fredriksen & Ørregaard Nielsen 2010) proposed to estimate the quadratic variation based on the continuous and jump components respectably as

$$CV_t = RV_t - JV_t, \quad t = 1, ..., T \tag{2.15}$$

$$JV_t = \sum_{i=1}^{M} JV_{t,i}, \quad t = 1, ..., T \tag{2.16}$$

where

$$JV_{t,i} = I_{\{\kappa_{t,i} \neq 0\}} \left(\kappa_{t,i}^2 - \frac{1}{m - M} \sum_{k \in \{1,...,m\} \setminus \{j_i,...,j_M\}} r_{t,k}^2 \right), \quad j = 1, ..., M,$$

is the quadratic variation increase for each intraday jump $\kappa_{t,i}$.

Chapter 3

Realized GARCH

In this section we consider the Realized generalized autoregressive conditional heteroskedasticity model (Realized GARCH) which was introduced by (Hansen et al. 2011), the notation used also follows from the same paper. The Realized GARCH model is closely related to the regular GARCH model, but incorporates realized measures of volatility, such as the realized variance shown in Eq.(2.6). In the GARCH(1,1) model the conditional variance, h_t, is a function of h_{t-1} and the squared returns r_{t-1}^2. Hence, the difference between the two models is the inclusion of a measurement equation, that relates the realized measures to the latent volatility. The general structure of the RealGARCH(p,q) model is given by,

$$\begin{aligned} r_t &= \sqrt{h_t} z_t, && (3.1)\\ h_t &= v(h_{t-1}, ..., h_{t-p}, x_{t-1}, ..., x_{t-q}), && (3.2)\\ x_t &= m(h_t, z_t, u_t), && (3.3) \end{aligned}$$

where $z_t \sim iid(0,1)$ and $u_t \sim iid(0, \sigma_u^2)$, with z_t and u_t being mutually independent. The first two equations we refer to as the *return equation* and the *GARCH equation*. These equations comes from the original GARCH-X models, where the x_t is treated as an exogenous variable. (Chen, Ghysels & Wang 2009) includes a list of such models and some related models.

The last equation, Eq. (3.3), we shall call the *measurement equation*, since the realized measure x_t introduced in this context can be interpreted as a measurement of the *GARCH equation*, h_t. This equation relates the realized measure to the returns, which in turn is found to be highly significant.

As an example the structure of a $RealGARCH(1,1)$ model is given below,

$$\begin{aligned} r_t &= \sqrt{h_t} z_t,\\ h_t &= \omega + \beta h_{t-1} + \gamma x_{t-1},\\ x_t &= \xi + \phi h_t + \tau(z_t) + u_t, \end{aligned}$$

where $h_t = var(r_t|F_{t-1})$ with $F_t = \sigma(r_t, x_t, r_{t-1}, x_{t-1}, ...)$. The standard GARCH model and other variants of ARCH is somewhat nested in the realized GARCH framework. (Bollerslev 2009) gives a list of such models. The following is two examples included by (Hansen et al. 2011) which shows how the realized GARCH is nested in the GARCH model and the EGARCH model by (Nelson 1991).

Substituting $x_t = r_t^2$ we can verify that the Realized GARCH(p,q) model nests the GARCH(p,q) model. With the parameters $p = q = 1$ we get the following GARCH(1,1) structure,

$$\begin{aligned} v(h_{t-1}, r_{t-1}^2) &= \omega + \alpha r_{t-1}^2 + \beta h_{t-1}, \\ m(h_t, z_t, u_t) &= h_t z_t^2 \end{aligned}$$

Where the measurement equation is simply an identity.

We can also obtain the EGARCH model by substituting $x_t = r_t$,

$$\begin{aligned} v(h_{t-1}, r_{t-1}) &= \exp\{\omega + \alpha|z_{t-1}| + \theta z_{t-1} + \beta \log h_{t-1}\}, \quad z_{t-1} = r_{t-1}/\sqrt{h_{t-1}}, \\ m(h_t, z_t, u_t) &= \sqrt{h_t} z_t \end{aligned}$$

In the next section we introduce the log-linear realized GARCH model.

3.1 Log-Linear Realized GARCH Specification

The log linear realized GARCH model is given by the following *GARCH equation* and *measurement equation*,

$$\log h_t = \omega + \sum_{i=1}^{p} \beta_i \log h_{t-i} + \sum_{j=1}^{q} \gamma_j \log x_{t-j}, \tag{3.4}$$

$$\log x_t = \xi + \phi \log h_t + \tau(z_t) + u_t, \tag{3.5}$$

where $z_t = r_t/\sqrt{h_t} \sim iid(0,1)$, $u_t \sim iid(0, \sigma_u^2)$ and $\tau(z)$ is the leverage function. The log-linear realized GARCH preserves the ARMA structure which can be extended to the standard GARCH models. This property gives the realized GARCH model certain advantages when comparing it to the standard GARCH model. (Hansen et al. 2011) gives a proposition which shows the GARCH equation with lagged squared returns. The GARCH equation is then given by the following equation,

$$\log h_t = \omega + \sum_{i=1}^{p} \beta_i \log h_{t-i} + \sum_{j=1}^{q} \gamma_j \log x_{t-j} + \sum_{j=1}^{q} \alpha_j \log r_{t-j}^2, \tag{3.6}$$

where $q = \max_i\{(\alpha_i, \gamma_i) \neq (0,0)\}$.

Proposition 1. *Define* $\omega_t = \tau(z_t) + u_t$ *and* $v_t = \log z_t^2 - \kappa$, *where* $\kappa = E \log z_t^2$. *The realized GARCH model defined by Eq.(15) and Eq.(17) implies*

$$\begin{aligned}
\log h_t &= \mu_h + \sum_{i=1}^{p\vee q}(\alpha_i + \beta_i + \phi\gamma_i)\log h_{t-i} + \sum_{j=1}^{q}(\gamma_j\omega_{t-j} + \alpha_j v_{t-j}),\\
\log x_t &= \mu_x + \sum_{i=1}^{p\vee q}(\alpha_i + \beta_i + \phi\gamma_i)\log x_{t-i} + \omega_t + \sum_{j=1}^{p\vee q}\{-(\alpha_j + \beta_j)\omega_{t-j} + \phi\alpha_j v_{t-j}\}\\
\log r_t^2 &= \mu_r + \sum_{i=1}^{p\vee q}(\alpha_i + \beta_i + \phi\gamma_i)\log r_{t-i}^2 + v_t + \sum_{j=1}^{p\vee q}\{\gamma_i(\omega_{t-j} - \phi v_{t-j}) - \beta_j v_{t-j}\},
\end{aligned}$$

where $\mu_h = \omega + \gamma_\bullet\xi + \alpha_\bullet\kappa$, $\mu_x = \phi(\omega + \alpha_\bullet\kappa) + (1 - \alpha_\bullet - \beta_\bullet)\xi$, *and* $\mu_r = \omega + \gamma_\bullet\xi + (1 - \beta_\bullet - \phi\gamma_\bullet)\kappa$, *with*

$$\alpha_\bullet = \sum_{j=1}^{q}\alpha_j, \quad \beta_\bullet = \sum_{i=1}^{p}\beta_i, \quad \textit{and} \quad \gamma_\bullet = \sum_{j=1}^{q}\gamma_j,$$

using the conventions $\beta_i = \gamma_j = \alpha_j = 0$ *for* $i > p$ *and* $j > q$.

This proposition gives the structure for the different realized GARCH equations. It implies that $\log h_t$ follows a $ARMA(p\vee q, q-1)$ structure, while $\log r_t^2$ and $\log x_t$ follows a $ARIMA(p\vee q, p\vee q)$ structure. The persistence of volatility is also given by the above proposition, such that,

$$\pi = \sum_{i=1}^{p\vee q}(\alpha_i + \beta_i + \phi\gamma_i) = \alpha_\bullet + \beta_\bullet + \phi\gamma_\bullet.$$

The LGARCH model which is the logarithmic GARCH model is closely nested in the log-linear framework see (Geweke 1986) and (Athreya & Pantula 1986).

3.2 The Leverage Function

In this section the leverage function will be introduced and discussed. The leverage effect is a well known phenomenon in stock markets of a negative correlation between today's return and tomorrow's volatility. So in the RealGARCH framework, the leverage function models the dependence between returns and tomorrows volatility. Hence, the parameters τ_1 and τ_2 introduced below, will give an indication of how dependent volatility are to changes in return. The function can be constructed based on different specifications. Based on the condition $E(\tau(z_t)) = 0$, a leverage function can be constructed by using the form

$$\tau(z_t) = \tau_1 a_1(z_t) + ... + \tau_k a_k(z_t), \quad \text{where} \quad E(a_k(z_t)) = 0, \forall k,$$

indicating that the function is linear in the unknown parameters. This functional form includes a broad class of leverage functions used in previous empirical analysis. In this paper we will concentrate on the hermite polynomials of the form

$$\tau(z) = \tau_1 z + \tau_2(z^2 - 1) + \tau_3(z^3 - 3z) + \tau_4(z^4 - 6z^2 + 3) + ...,$$

(Hansen et al. 2011) showed that if more then the two terms of highest order in the leverage function was included, then those would become insignificant. Hence, the leverage function we consider will be a simple quadratic form, such as

$$\tau(z_t) = \tau_1 z_t + \tau_2(z_t^2 - 1)$$

This polynomial gives a simplified expression for the asymmetries in the leverage function which is similar to the EGARCH model (Nelson 1991). These asymmetries captures the slope of the news impact curve which is introduced in the next section. Hence, the asymmetries are summarized by the statistics,

$$\rho^- = corr\{\tau(z_t) + u_t | z_t > 0\} \quad \text{and} \quad \rho^+ = corr\{\tau(z_t) + u_t | z_t < 0\}.$$

3.3 News impact curve

The leverage function introduced in the previous section is closely related to the news impact curve which will be presented in this section. The news impact curve was first introduced by (Engle & Ng 1991) and shows how volatility is impacted by shocks to the price. (Chen & Ghysels 2010) gives a detailed study of the news impact curve with the use of high frequency data. The estimation of the news impact curve are simplified with the use of a leverage function with hermite polynomial form. Assuming a realized GARCH model with a log-linear specification we can define the news impact curve by,

$$\nu(z) = E(\log h_{t+1} | z_t = z) - E(\log h_{t+1}),$$

which again implies that the percentage impact on volatility can be represented by $100\nu(z)$. Since the realized GARCH model can be represented with a ARIMA structure, we have that $\nu(z) = \gamma_1 \tau(z_t)$.

3.4 Quasi-Maximum Likelihood Analysis

In this section the properties of the quasi-maximum likelihood estimator related to the *Realized GARCH(p,q)* model is discussed. The relation between the *Realized GARCH(p,q)* model and the original GARCH model was shown to be significant. This in turn can also be said about the structure of the QMLE analysis. One of the basic ideas is that both the *GARCH equation* and the *measurement equation* are taken to be independent formulations of the likelihood function. This result in a likelihood function that can be used to compare the $GARCH(p,q)$ model to the more sophisticated *Realized* $GARH(q,p)$ model which will be presented later.

In this section the underlying QMLE structure for the log-linear Realized GARCH model will be represented. Both the score and the Hessian will be given and the regularity conditions will be discussed. The log likelihood function, where a Gaussian specification is assumed, is given by,

$$l(r,x;\theta) = -(\frac{1}{2})\sum_{t=1}^{n}[\log(h_t) + \frac{r_t^2}{h_t} + \log(\sigma_u^2) + \frac{u_t^2}{\sigma_u^2}]$$

Where the leverage function is represented as $\tau' a_t = \tau_1 a_1(z_t) + ... + \tau_k' a_k(z_t)$, and the parameters in the model is given as,

$$\theta = (\lambda', \psi', \sigma_u^2)' \quad and \quad \lambda = (\omega, \beta_1, ..., \beta_p, \gamma_1, ..., \gamma_q)' \quad \psi = (\xi, \phi, \tau')'$$

Both the GARCH and measurement equations can be simplified by writing $\widehat{h_t} = \log(h_t)$, $\widehat{x_t} = log(x_t)$ and express the equations as,

$$g_t = (1, \widehat{h}_{t-1}, ..., \widehat{h}_{t-p}, \widehat{x}_{t-1}, ..., \widehat{x}_{t-q})', \quad m_t = (1, \widehat{h}_t, a_t')'.$$

where

$$\widehat{h}_t = \lambda' g_t \quad and \quad \widehat{x}_t = \psi' m_t + u_t$$

Next, both the score and the Hessian is represented as derivatives with respect to λ. The next Lemma and proposition is taken from (Hansen et al. 2011).

Lemma 1. *Define* $\dot{h}_t$ *and* $\ddot{h}_t = \frac{\partial^2 \widehat{h}_t}{\partial\lambda\partial\lambda'}$. *Then* $\dot{h}_s = 0$ *and* $\ddot{h}_s = 0$ *for* $s \leq 0$, *and*

$$\dot{h}_t = \sum_{i=1}^{p} \beta_i \dot{h}_{t-i} + g_t \quad and \quad \ddot{h}_t = \sum_{i=1}^{p} \beta_i \ddot{h}_{t-i} + (\dot{H}_{t-1} + \dot{H}_{t-1}'),$$

where $\dot{H}_{t-1} = (0_{1+p+q\times 1}, \dot{h}_{t-1}, ..., \dot{h}_{t-p}, 0_{1+p+q\times q})$ *is an* $p+q+1 \times p+q+1$ *matrix.*
(ii) When $p = q = 1$ *we have with* $\beta = \beta_1$ *that*

$$\dot{h}_t = \sum_{j=0}^{t-1} \beta^j g_{t-j} \quad and \quad \ddot{h}_t = \sum_{k=1}^{t-1} k\beta^{k-1}(G_{t-k} + G_{t-k}'),$$

where $G_t = (0_{3\times 1}, g_t, 0_{3\times 1})$.

Proposition 2. *(i) The score,* $\frac{\partial l}{\partial\theta} = \sum_{t=1}^{n} \frac{\partial l_t}{\partial\theta}$, *is given by*

$$\frac{\partial l_t}{\partial\theta} = -\frac{1}{2}\begin{pmatrix} (1 - z_t^2 + \frac{2u_t}{\sigma_u^2}\dot{u}_t)\dot{h}_t \\ -\frac{2u_t}{\sigma_u^2} m_t \\ \frac{\sigma_u^2 - u_t^2}{\sigma_u^4} \end{pmatrix}$$

where $\dot{u}_t = \frac{\partial u_t}{\partial \log h_t} = -\phi + \frac{1}{2} z_t \tau' \dot{a}_t$ *with* $\dot{a}_t = \frac{\partial a(z_t)}{\partial z_t}$.
(ii) The second derivative, $\frac{\partial^2 l}{\partial\theta\partial\theta'} = \sum_{t=1}^{n} \frac{\partial^2 l_t}{\partial\theta\partial\theta'}$, *is given by*

$$\frac{\partial^2 l_t}{\partial\theta\partial\theta'} = \begin{pmatrix} -\frac{1}{2}\{z_t^2 + \frac{2(\dot{u}_t^2 + u_t\ddot{u}_t)}{\sigma_u^2}\}\dot{h}_t\dot{h}_t' - \frac{1}{2}\{1 - z_t^2 + \frac{2u_t\dot{u}_t}{\sigma_u^2}\}\ddot{h}_t & \bullet & \bullet \\ \frac{\dot{u}_t}{\sigma_u^2}m_t\dot{h}_t' + \frac{u_t}{\sigma_u^2}b_t\dot{h}_t' & -\frac{1}{\sigma_u^2}m_t m_t' & \bullet \\ \frac{u_t\dot{u}_t}{\sigma_u^4}\dot{h}_t' & \frac{u_t}{\sigma_u^4}m_t' & \frac{1}{2}\frac{\sigma_u^2 - 2u_t^2}{\sigma_u^6} \end{pmatrix}$$

where $b_t = (0, 1, -\frac{1}{2}z_t\dot{a}_t')$ *and* $\ddot{u}_t = -\frac{1}{4}\tau'\{z_t\dot{a}_t + z_t^2\ddot{a}_t\}$ *with* $\ddot{a}_t = \partial^2 a(z_t)/\partial z_t^2$.

An important aspect of time series models is the stationary representation. Considering the above lemma and proposition, (Carrasco & Chen 2002) introduced a proposition which can be used in this context. They stated that if $\pi = \beta + \phi\gamma \in (-1, 1)$ then $\widehat{h}_t$ has a stationary representation. This condition can easily be obtained trough an linear constrained optimization algorithm. For calculation of standard errors, Proposition 3 in (Hansen et al. 2011) states that if $\{(r_t, x_t, \widehat{h}_t)\}$ is stationary and ergodic, then

$$\frac{1}{\sqrt{n}}\sum_{t=1}^{n}\frac{\partial l_t}{\partial\theta} \xrightarrow{d} N(0, J_\theta) \quad and \quad -\frac{1}{n}\sum_{t=1}^{n}\frac{\partial^2 l_t}{\partial\theta\partial\theta'} \xrightarrow{p} I_\theta$$

provided that

$$J_\theta = \begin{pmatrix} \frac{1}{4}E(1 - z_t^2 + \frac{2u_t}{\sigma_u^2}\dot{u}_t)^2 E(\dot{h}_t\dot{h}_t') & \bullet & \bullet \\ -\frac{1}{\sigma_u^2}E(\dot{u}_t m_t\dot{h}_t') & \frac{1}{\sigma_u^2}E(m_t m_t') & \bullet \\ -\frac{E(u_t^3)E(\dot{u}_t)}{2\sigma_u^6}E(\dot{h}_t') & \frac{E(u_t^3)}{2\sigma_u^6}E(m_t') & \frac{E(u_t^2/\sigma_u^2 - 1)^2}{4\sigma_u^4} \end{pmatrix}$$

and

$$I_\theta = \begin{pmatrix} \{\frac{1}{2} + \frac{E(\dot{u}_t^2)}{\sigma_u^2}\}E(\dot{h}_t\dot{h}_t') & \bullet & 0 \\ -\frac{1}{\sigma_u^2}E\{(\dot{u}_t m_t + u_t b_t)\dot{h}_t'\} & \frac{1}{\sigma_u^2}E(m_t m_t') & 0 \\ 0 & 0 & \frac{1}{2\sigma_u^4} \end{pmatrix}$$

are finite. Using these propositions results in a model only valid for the stationary case $\pi < 1$. For a more analytical approach the reader is refer to the appendix in (Hansen et al. 2011).

3.5 Direct computation of standard errors

Standard errors can be obtained from numerical derivatives, but can also be computed directly. By using the score and hessian the standard errors can be represented as,

$$\hat{J} = \frac{1}{n}\sum_{t=1}^{n}\hat{s}_t\hat{s}_t^{'}, \quad where \quad \hat{s}_t = \left\{\frac{1}{2}(1 - \hat{z}_t^2 + \frac{2\hat{u}_t}{\hat{\sigma}_u^2}\hat{u}_t)\hat{h}_t^{'}, -\frac{\hat{u}_t}{\hat{\sigma}_u^2}\hat{m}_t^{'}, \frac{\hat{\sigma}_u^2 - \hat{u}_t^2}{2\hat{\sigma}_u^4}\right\}'$$

and

$$\hat{I} = \frac{1}{n}\sum_{t=1}^{n}\begin{pmatrix} \frac{1}{2}\left\{\hat{z}_t^2 + \frac{2(\hat{u}_t^2+\hat{u}_t\hat{u}_t)}{\hat{\sigma}_u^2}\right\}\hat{\dot{h}}_t\hat{\dot{h}}_t' + \frac{1}{2}\left\{1-\hat{z}_t^2+\frac{2\hat{u}_t\hat{u}_t}{\hat{\sigma}_u^2}\right\}\hat{\ddot{h}}_t & \bullet & \bullet \\ -\hat{\sigma}_u^{-2}(\hat{u}_t\hat{m}_t+\hat{u}_t\hat{b}_t)\hat{\dot{h}}_t' & \frac{1}{\hat{\sigma}_u^2}\hat{m}_t\hat{m}_t' & \bullet \\ -\frac{\hat{u}_t\hat{u}_t}{\hat{\sigma}_u^4}\hat{\dot{h}}_t' & -\frac{\hat{u}_t}{\hat{\sigma}_u^4}\hat{m}_t' & \frac{1}{2}\frac{2\hat{u}_t^2-\hat{\sigma}_u^2}{\hat{\sigma}_u^6} \end{pmatrix}$$

$$= \frac{1}{n}\sum_{t=1}^{n}\begin{pmatrix} \frac{1}{2}\left\{\hat{z}_t^2 + \frac{2(\hat{u}_t^2+\hat{u}_t\hat{u}_t)}{\hat{\sigma}_u^2}\right\}\hat{\dot{h}}_t\hat{\dot{h}}_t' + \frac{1}{2}\left\{1-\hat{z}_t^2+\frac{2\hat{u}_t\hat{u}_t}{\hat{\sigma}_u^2}\right\}\hat{\ddot{h}}_t & \bullet & \bullet \\ -\hat{\sigma}_u^{-2}(\hat{u}_t\hat{m}_t+\hat{u}_t\hat{b}_t)\hat{\dot{h}}_t' & \frac{1}{\hat{\sigma}_u^2}\hat{m}_t\hat{m}_t' & \bullet \\ -\frac{\hat{u}_t\hat{u}_t}{\hat{\sigma}_u^4}\hat{\dot{h}}_t' & 0 & \frac{1}{\hat{\sigma}_u^4} \end{pmatrix}$$

such that the zero condition follows from $\sum_{t=1}^{n}\hat{u}_t\hat{m}_t' = 0$. The above method follows from the fisher information, such that the standard errors can be computed based on asymptotic properties.

3.6 Standard GARCH model related to the Real-GARCH model

The previous section introduced the log-likelihood function for the RealGARCH model. This function can be expressed as

$$\log L((\{r_t, x_t\})_{t=1}^n;\theta) = \sum_{t=1}^{n}\log f(r_t, x_t|F_{t-1}),$$

where r_t are the returns, x_t are the realized measure and F_t is the information given for $t \geq 0$. The realized measure expressed in the log-likelihood is not present in the standard GARCH model, so we need to rewrite the likelihood function to be able to compare these models. This can be done by factorizing the join conditional density for (r_t, x_t) by

$$f(r_t, x_t|F_{t-1}) = f(r_t|F_{t-1})f(x_t|r_t, F_{t-1})$$

This factorization gives us, by inspection, the possibility to split the joint likelihood into the sum, such that

$$l(r,x) = -\frac{1}{2}\sum_{t=1}^{n}[\log(2\pi)+\log(h_t)+\frac{r_t^2}{h_t}] + -\frac{1}{2}\sum_{t=1}^{n}[\log(2\pi)+\log(\sigma_u^2)+\frac{u_t^2}{\sigma_u^2}] \quad (3.7)$$

So the first part of Eq.(3.7) is equal to the log-likelihood specification for the standard logarithmic GARCH model. This can then be used to compare the standard logarithmic GARCH model to the log-linear Realized GARCH model.

3.7 Distributions

The Realized GARCH model initially assumes a Gaussian distribution for both z_t and u_t/σ_u. In this section we introduce other possible distributions for the standardized error term z_t in Eq. (3.1). (Hansen 1994) introduced a flexible density function which incorporates both heavy tails and skewness. The density functions which will be represented here also have closed form solutions which facilitates quasi-likelihood estimation. The first density function we introduce is a generalization of the student's t distribution with normalized unit variance,

$$g(z|\nu) = \frac{\Gamma\left(\frac{\nu+1}{2}\right)}{\sqrt{\pi(\nu-2)}\Gamma\left(\frac{\nu}{2}\right)}\left(1+\frac{z^2}{(\nu-2)}\right)^{-(\nu+1)/2}$$

where $2 < \nu < \infty$. The student's t distribution is less restrictive then the Gaussian distribution, allowing for variation in the parameters. Considering that the realized GARCH model produces returns with access skewness, the skewed student's t distribution might be a natural extension to the regular student's t distribution. (Hansen 1994) introduced the following density function which allows for restrictions for the different parameters.

$$g(z|\nu,\epsilon) = \begin{cases} bc\left(1+\frac{1}{\nu-2}\left(\frac{bz+a}{1-\epsilon}\right)^2\right)^{-(\nu+2)/2} & \text{if } z < -\frac{a}{b} \\ bc\left(1+\frac{1}{\nu-2}\left(\frac{bz+a}{1+\epsilon}\right)^2\right)^{-(\nu+2)/2} & \text{if } z \geq -\frac{a}{b} \end{cases} \tag{3.8}$$

where $2 < \nu < \infty$. and $-1 < \epsilon < 1$. The constants a, b, and c, are given by

$$a = 4\epsilon c\left(\frac{\nu-2}{\nu-1}\right), \qquad b^2 = 1+3\epsilon^2-a^2,$$

$$c = \frac{\Gamma\left(\frac{\nu+1}{2}\right)}{\sqrt{\pi(\nu-2)}\Gamma\left(\frac{\nu}{2}\right)}$$

The reader is referred to the Appendix in (Hansen 1994) for the proof that this is a proper density function and it facilitates mean zero and unit variance, which is important in the ARCH framework. By substituting $\epsilon = 0$ in Eq.(3.8) the density function reduces to the standard student's t distribution and by setting $\epsilon = 0$ and $\nu = \infty$ we obtain the Gaussian distribution. If the skewness parameter ϵ is greater then zero, the distribution mode is to the left of zero and distribution is skewed to the right, and the opposite is true for ϵ less then zero.

Figure 3.1 represents the theoretical distributions for the above density functions with zero mean and unit variance. The skewness and scale parameters are only for

a visual representation and does not connect to the result.

Since the distributions only applies to the standardized error term z_t, the measurement equation will be unchanged. The same factorization used for the log-likelihood is then valid, such that

$$L = \prod_{t=1}^{n} h(r_t|x_1, ..., x_{t-1}) l(x_t|x_1, ..., x_{t-1}, r_t)$$

where $h(r_t|x_1, ..., x_{t-1})$ is determined by the distribution of z_t and $l(x_t|x_1, ..., x_{t-1}, r_t)$ is the normal distribution with mean $\mu + \phi \log \sigma_t^2 + \tau(z_t)$ and variance σ_u^2. Introducing a new distribution for z_t only changes the log-likelihood for $h(..)$ and keeps $l(..)$ unchanged. As an example of a valid log-likelihood (Lambert & Laurent 2000, Lambert & Laurent 2002) introduced an extension of the skewed student's t density which was proposed by (Fernández & Steel 1998).

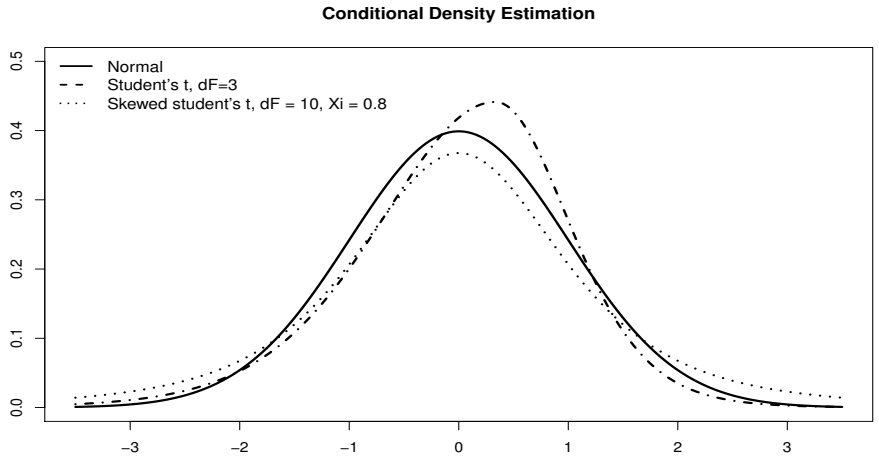

Figure 3.1: *Density functions with zero mean and unit variance. The density functions represented are the standard normal, student's t with 3 degrees of freedom and skewed student's t distributions with 10 degrees of freedom and skew parameter 0.8.*

$$G(z_t|\nu) = \frac{\Gamma((\nu+1)/2)}{\Gamma(\nu/2)\sqrt{\pi(\nu-2)}} \left(1 + \frac{z_t^2}{\nu-2}\right)^{-(\nu+1)/2}$$

where $z_t = r_t/h_t$, $\Gamma(\nu) = \int_0^\infty e^{-x} x^{\nu-1} \mathrm{d}x$ is the gamma function and, ν is the parameter that measures the tail thickness. By introducing the density into the

GARCH framework the log-likelihood can be represented by,

$$\begin{aligned} L_{sst}(r_t|x_t,\epsilon,\nu) = & - \frac{1}{2}\sum_{t=1}^{n}\Bigg[\log\Gamma\left(\frac{\nu+1}{2}\right) - \log\Gamma\left(\frac{\nu}{2}\right) - \frac{1}{2}\log(\pi(\nu-2)) \\ & + \log\left(\frac{2}{\epsilon+(1/\epsilon)}\right) + \log(s) - \frac{1}{2}\log(h_t) + (1+\nu) \\ & \log\left(1+\frac{(sz_t+m)^2}{\nu-2}\epsilon^{-2\mathbf{I_t}}\right) - \frac{1}{2}\log(2\pi) + \log(\sigma_u^2) + \frac{u_t^2}{\sigma_u^2}\Bigg] \end{aligned}$$

where ϵ is the asymmetry parameter and ν is the degree of freedom for the distribution. The distribution related to the measurement equation remains unchanged while the skewed student's t distribution has been incorporated for the GARCH equation. The parameters m and s is represented as,

$$m = \frac{\Gamma(\frac{\nu-1}{2})\sqrt{\nu-2}}{\sqrt{\pi}\Gamma(\frac{\nu}{2})}\left(\epsilon - \frac{1}{\epsilon}\right), \qquad s^2 = \left(\epsilon^2 + \frac{1}{\epsilon^2} - 1\right) - m^2$$

with the indicator function $\mathbf{I_t}$ given as,

$$\mathbf{I_t} = \begin{cases} 1, & \text{if} \quad z_t \geq -\frac{m}{s} \\ -1 & \text{if} \quad z_t < -\frac{m}{s} \end{cases}$$

The log-likelihood for the generalized student's t distribution follows from the skewed student's t distribution.

$$\begin{aligned} L_{st}(r_t|x_t,\nu) = & - \frac{1}{2}\sum_{t=1}^{n}\Bigg[\log\Gamma\left(\frac{\nu+1}{2}\right) - \log\Gamma\left(\frac{\nu}{2}\right) - \frac{1}{2}\log(\pi(\nu-2)) \\ & - \frac{1}{2}\log(h_t) + (1+\nu)\log\left(1+\left(\frac{z_t^2}{\nu-2}\right)\right) \\ & - \frac{1}{2}\log(2\pi) + \log(\sigma_u^2) + \frac{u_t^2}{\sigma_u^2}\Bigg] \end{aligned}$$

Chapter 4

Empirical Results

In this section we present empirical results for the quadratic variation theory and the realized GARCH model. The results are based on intraday returns for the ICE Brent Crude Oil future front month contract. Detailed results are represented for 3, 5, 10, 15 and 30 minute observation frequencies together with stylized facts for the intraday returns and realized measures. We estimate the realized GARCH model based on the five different frequencies. A more detailed study is done for the 3 minute realized variance with the inclusion of distributions for the standardized error term and comparison to the logarithmic GARCH model.

In this paper we use the log-linear realized GARCH(1,2) model. (Hansen et al. 2011) states that the log-linear realized GARCH model is far less miss-specified then the linear model. They show this by comparing robust and non-robust standard errors. The model can be represented as,

$$\begin{aligned} r_t &= \sqrt{h_t} z_t \\ h_t &= \exp\{\omega + \beta \log h_{t-1} + \gamma_1 \log x_{t-1} + \gamma_2 \log x_{t-2}\} \\ \log x_t &= \xi + \phi \log h_t + \tau(z_t) + u_t \end{aligned}$$

We parametrize the model by setting $p = 1$ and $q = 2$, indicating that h_t and x_t are included with one and two lags respectively. The parameters are based on results where we found small, but statistical significant evidence for the realized GARCH(1,2) model compared to the realized GARCH(1,1) model. The statistic used was the likelihood ratio statistic where each of the three smaller models are benchmarked against the largest model. In the QMLE framework the distribution for the likelihood ratio, LR_i, is given as a weighted sum of χ^2-distributions [1].

[1] The likelihood ratio statistic given as,

$$LR_i = 2\{l_{RG(p,q)}(r,x) - l_i(r,x)\},$$

is only a indicator of significance.

4.1 Data description

In this section we discuss the contract specifications for the ICE Brent Crude Futures and the data connected to these contracts. These are deliverable contracts based on EFP [2] delivery with an option to cash settle. The contracts span a maximum of 72 consecutive months with addition to 6 contract months comprising of June to December which will be listed for an additional three calender years. In this paper we take a closer look at the front month contract. This contract span one month with expiration date either on the 15th day before the first day of the contract month or if the 15th is not a business day, the next proceeding business day. Trading hours are based on UK hours with open 01:00 London local time and close 22:00 London local time. The settlement price for the contract are based on the weighted average price for trades during a three minute settlement period from 19:27:00, London time. The trading hours reported in this paper refers to London local time, indicating that EST opens at 20:00, Chicago opens at 19:00 and Singapore opens at 08:00. The data used in this paper contains information

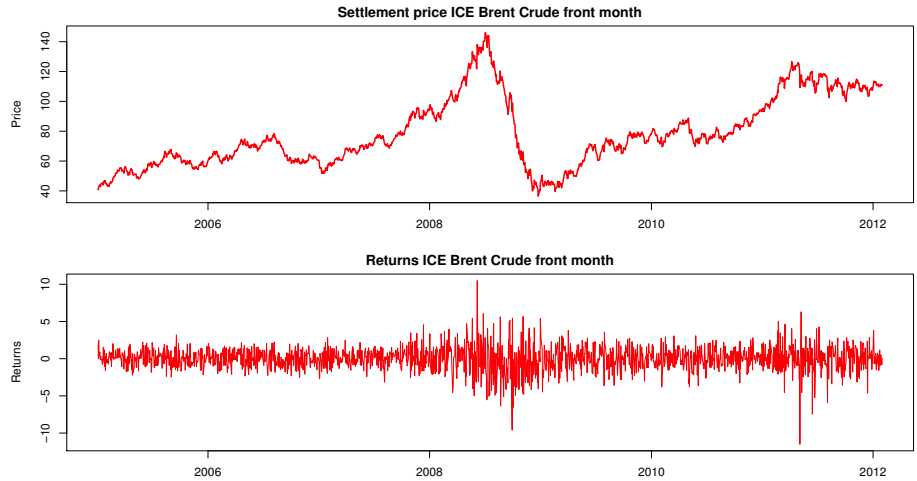

Figure 4.1: *The figure shows settlement prices and returns for the ICE Brent Crude front month contract for the period 1/1/2005 to 31/1/2012. The settlement price used for both figures are based on a weighted average price during a three minute settlement period from 19:27:00, London local time.*

regarding every trade and/or quotation in the period 1/1/2005 to 31/1/2012. For liquidity reasons, only the front month contract was taken into consideration when constructing the time series. Previous empirical results has shown that the time step between intraday returns should depend on the liquidity and micro structure noise in the traded contract. In other words, if the liquidity is low (low trading frequency) the time step between intraday returns should be increased. This results in a better representation of the realized variance which limits the possibility for

[2]The Exchange of Futures for Physical (EFP) is an alternative mechanism that is used to price physical crude oil. Participants can exchange their future positions for a physical position.

overestimation. In this paper we operate with five different observation frequencies. Hence, prices are recorded with 3, 5, 10, 15 and 30 minute step sizes which results in 421, 253, 127, 85 and 43 intraday observations respectively. Returns are calculated based on weighted average trades between 19:27 and 19:30 London local time. Figure 4.1 shows settlement prices and returns for the ICE Brent Crude front month contract for the period 1/1/2005 to 31/1/2012.

Table 4.1 Panel A-E shows the descriptive statistics of daily intraday returns where each Panel refers to the frequency of intraday returns. The mean for the total sample in Panel A-E is not significantly different from zero. The min and max ranges from -4.5 to 3.3 for the total sample in all the Panels. Overall the biggest returns are recorded in Panel E where the 30 minute returns are given. The standard deviation increases together with the frequency off observations. The skewness for all the total samples are significantly above zero and the kurtosis is high and increasing together with the observation frequency. This shows that the distribution of the intraday returns is leptokurtic.

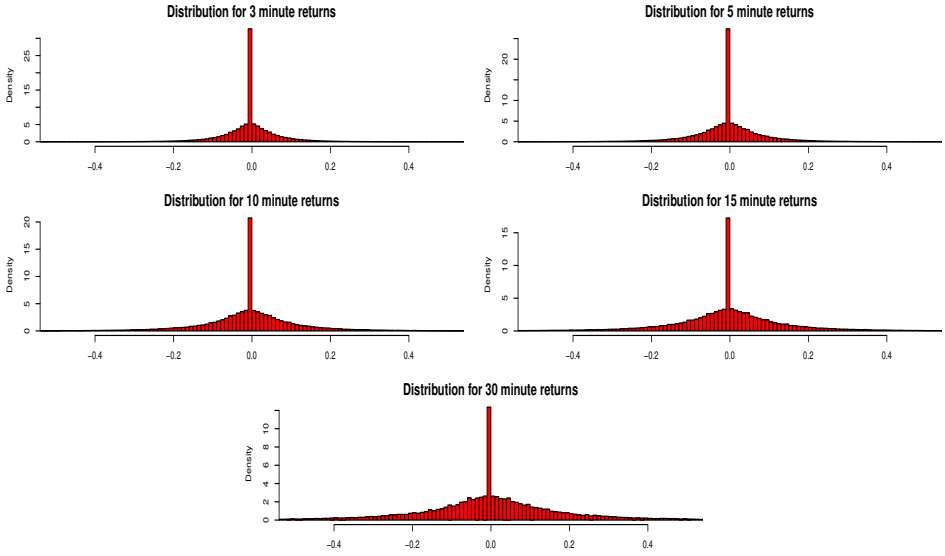

Figure 4.2: *The figure shows distributions for 3, 5, 10, 15 and 30 minute returns based on the ICE Brent Crude Oil Future front month contract. The observation frequencies has 421, 253, 127, 85 and 43 intraday returns respectively. The data is taken from the period 1/1/2005 to 31/1/2012.*

The Jarque-Bera (JB) statistic which incorporates both the skewness and the kurtosis rejects the null hypothesis of normality at the 1% significance level for all samples. Figure 4.2 shows distributions for 3, 5, 10, 15 and 30 minute returns. The figure indicate that there is a high amount of zero returns for all the total samples, but the densities suggests that there is a high reduction in zero returns

from 3 to 30 minute returns. Hence, the assumption of normal distributed intra-day returns are rejected. The Ljung-Box statistic, $Q(10)$ and $Q2(10)$, tests the null hypothesis that there is no correlation up to lag 10. This test was done for regular returns, $Q(10)$, and squared returns, $Q2(10)$. The Ljung-Box statistic rejects the null hypothesis for all the total series at the 1 % significance level both for regular returns and squared returns. The time of day series shows some correlation for the different observation frequencies, but does not behave in any particular pattern.

Figure 4.3 gives a visual representation of the correlation in the total sample series for the different frequencies. The regular returns shows low correlation for all the total samples. Persistence in volatility is shown in the auto correlation of squared returns. Indicating that the correlation for squared returns are significantly higher then for regular returns.

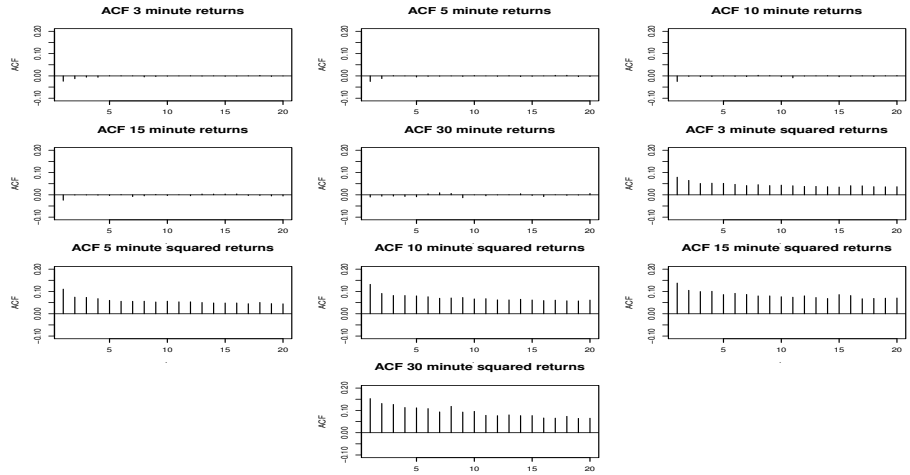

Figure 4.3: *The Figure shows auto correlation for 3, 5, 10, 15 and 30 minute returns and squared returns from the ICE Brent Crude Oil Future front month contract. The correlation is calculated using the full sample sizes.*

Panel A: Descriptive Statistics for 3 minute returns										
	#obs	Mean	Min	Max	St.Dev.	Skew	Kurt	JB^3	$Q(10)$	$Q2(10)$
Total[1]	$760k^2$	0.00	-4.5	3.3	0.04	1.97	91.98	1.9e8	646.0^{***}	13241^{***}
02:30	1804	0.00	-0.75	1.22	0.05	6.01	216.2	3.4e6	3.58	0.139
06:30	1804	0.00	-0.62	0.57	0.05	-0.16	28.05	4.7e4	27.11^{***}	45.31^{***}
10:30	1804	0.00	-0.7	1.08	0.08	0.81	33.65	7.1e4	11.61	2.02
14:30	1804	0.01	-0.61	0.78	0.12	0.40	7.916	1.8e3	25.46^{***}	137.7^{***}
20:30	1804	0.00	-0.46	0.38	0.05	-1.01	22.83	2.9e5	16.94^{*}	24.4^{***}
Panel B: Descriptive Statistics for 5 minute returns										
	#obs	Mean	Min	Max	St.Dev.	Skew	Kurt	JB^3	$Q(10)$	$Q2(10)$
Total[1]	$456k^2$	0.00	-4.5	3.3	0.05	3.42	89.21	5.5e7	378.3^{***}	12628^{***}
02:30	1804	0.00	-0.75	1.22	0.06	3.86	110.9	8.8e5	17.7^{*}	4.02
06:30	1804	0.00	-0.98	0.49	0.07	-1.63	32.78	6.7e4	19.34^{**}	17.3^{*}
10:30	1804	0.00	-1.49	1.37	0.10	-0.78	48.66	1.6e5	11.46	5.45
14:30	1804	0.01	-0.68	0.86	0.15	0.61	7.427	1.5e3	11.35	122^{***}
20:30	1804	0.00	-1.2	0.48	0.07	-3.55	64.76	2.9e5	19.31^{**}	1.24
Panel C: Descriptive Statistics for 10 minute returns										
	#obs	Mean	Min	Max	St.Dev.	Skew	Kurt	JB^3	$Q(10)$	$Q2(10)$
Total[1]	$229k^2$	0.00	-4.5	3.3	0.06	1.06	45.64	1.2e7	160.8^{***}	8492^{***}
02:30	1804	0.00	-0.75	1.22	0.08	1.62	47.69	1.5e5	17.8^{*}	8.02
06:30	1804	0.00	-1.24	0.57	0.09	-1.49	28.66	5.0e4	25.8^{***}	27.12^{***}
10:30	1804	0.01	-0.76	1.08	0.13	0.145	10.71	4.5e3	25.1^{***}	48.93^{***}
14:30	1804	-0.01	-3.09	1.85	0.29	-1.59	29.98	5.5e4	26.8^{***}	39.36^{***}
20:30	1804	0.00	-1.32	0.6	0.09	-2.31	47.42	1.5e5	9.98	4.78
Panel D: Descriptive Statistics for 15 minute returns										
	#obs	Mean	Min	Max	St.Dev.	Skew	Kurt	JB^3	$Q(10)$	$Q2(10)$
Total[1]	$153k^2$	0.00	-4.5	3.3	0.07	2.88	40.77	4.8e6	108.6^{***}	6756^{***}
02:30	1804	0.00	-0.75	1.22	0.10	0.68	27.82	4.6e4	20.9^{**}	5.83
06:30	1804	0.01	-1.21	0.84	0.11	-1.22	24.39	3.4e4	35.5^{***}	76.54^{***}
10:30	1804	0.01	-1.28	0.9	0.15	-0.07	9.81	3.4e3	12.4	67.49^{***}
14:30	1804	0.01	-1.34	1.64	0.25	0.17	6.864	1.1e3	10.9	123^{***}
20:30	1804	0.00	-1.35	1.02	0.11	-0.76	35.35	7.4e4	15.7	27.2^{***}
Panel E: Descriptive Statistics for 30 minute returns										
	#obs	Mean	Min	Max	St.Dev.	Skew	Kurt	JB^3	$Q(10)$	$Q2(10)$
Total[1]	$77k^2$	0.00	-4.5	3.3	0.10	1.69	12.63	1.1e6	50.2^{***}	4280^{***}
02:30	1804	0.00	-1.43	1.22	0.15	-0.69	19.40	2.0e4	11.7	46.1^{***}
06:30	1804	0.01	-1.46	0.94	0.15	-0.93	15.63	1.2e4	17.8^{*}	165^{***}
10:30	1804	0.02	-1.72	1.41	0.23	-0.24	9.819	3.4e3	57.2^{***}	174^{***}
14:30	1804	0.01	-2.08	1.77	0.36	-0.17	6.295	8.2e2	20.12^{**}	321.8^{***}
20:30	1804	0.00	-1.38	0.96	0.13	-0.30	18.25	1.7e4	34.1^{***}	31.46^{***}

[1] Total sample of observation. [2] k is equal to thousand. [3] Jarque-Bera test statistic.

Table 4.1: *Descriptive statistics for the ICE Brent Crude future contracts with 3,5,10,15 and 30 minute intraday returns. The table shows number of observations, mean, min, max, standard deviation, skewness, kurtosis, JB is the Jarque-Bera statistic to test the null hypothesis of normality, Q(10) is the Ljung-Box statistic adjusted for heteroskedasticity following (Diebold 1988) to test the null hypothesis of no autocorrelations up to 10 lags and Q2(10) is the same test, but used for squared returns. The tests are done for the total sample and all returns recorded at 02:30, 06:30, 10:30, 14:30 and 20:30 for each day. *** Rejected at the 1 % significance level. ** Rejected at the 5 % significance level. * Rejected at the 10 % significance level.*

4.2 Stylized Facts For Intraday Returns

It has been shown that high-frequency prices and returns can improve volatility estimates and forecasts. In this section we discuss some stylized facts related to intraday returns. These facts are discussed in more detail by (Taylor 2007). With the inclusion of high-frequency data, prices can be analyzed down to every trade and/or quotation. This involves some difficulty since the buy and sell quotes differ, the time between tick observations varies and there are enormous amounts of data. Because of these restrictions the prices has to be observed at some intermediate frequency. This is typically every five minutes, but varies based on frequency of trading. Figure 4.4 shows a typical day where each dot refers to a specific price, recorded each 3 minutes. On this specific day there was five trade, on average,

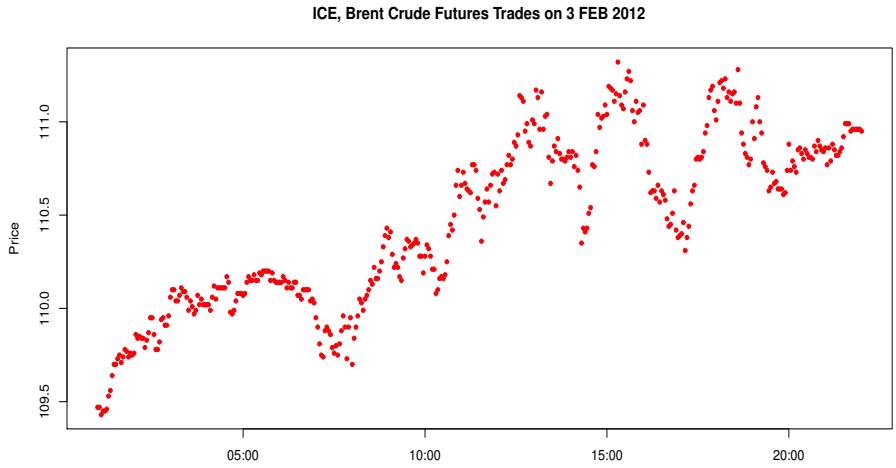

Figure 4.4: *ICE Berent Crude Futures trades where prices are recorded each 3 minutes. Prices are recorded from opening hour, 01:00, until close at 22:00 GMT.*

every second. The returns obtained from each price observation have a fat-tailed distribution which again corresponds to a high kurtosis. (Taylor 2007) gives a list of some stylized facts that was found to be correct for the intraday returns obtained from the ICE Brent Crude Futures contracts.

- Returns obtained from intraday observations have a fat-tailed distribution, with increasing kurtosis for higher observation frequency.
- Returns from intraday observations are almost uncorrelated. Any important dependence is usually negative and between consecutive returns.
- There is substantial positive dependence among intraday absolute returns. It occurs at many low lags.
- The level of volatility on average depends on time of day, with a significant intraday variation.

The last point refers to volatility patterns that depend on time during the day, the day of week and macroeconomic news announcements. Figure 4.5 summerises the intraday pattern for the ICE Brent Crude Future market across all days of the week, from 1/1/2005 to 31/1/2012. The returns are based on three-minutes returns from open, 01:00 to close at 22:00 GMT. It's important to note that a circular is issued when the UK switches from GMT to BST and also when the US switches from DST which will affect the closing times. This is also shown in Figure 4.5, indicating that the two last spikes refers both to contract changes. In section 2 we

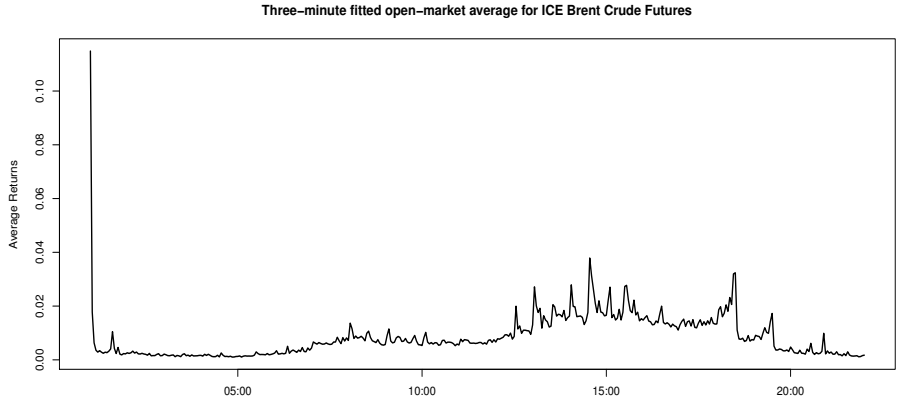

Figure 4.5: *Three-minute fitted open-market average returns for the ICE Brent Crude Future contracts, using all days of the week, for the period 1/1/2005 to 31/1/2012.*

introduced a fairly accurate measure of volatility, known as realized volatility. In this paper we operate with five different frequencies for realized volatility, defined by

$$RV_t = \sqrt{\sum_{j=1}^{N} r_{t,j}^2}$$

where N is dependent on which observation frequency is used. Realized volatility also exhibits some stylized facts which is found true for many markets (Taylor 2007).

- The distribution, trough time, of RV_t is approximately log normal. See Figure 4.6 a), where the dotted cure is the theoretical log normal distribution.
- The distribution of daily returns divided by realized volatility, i.e of r_t/RV_t, is approximately normal, unlike the distribution of returns. See Figure 4.6 b), where the dotted curve is the theoretical normal distribution.
- The autocorrelation of realized volatility (and its logarithm) decay slowly and resembles those of a "long memory" process. See Figure 4.6 c).

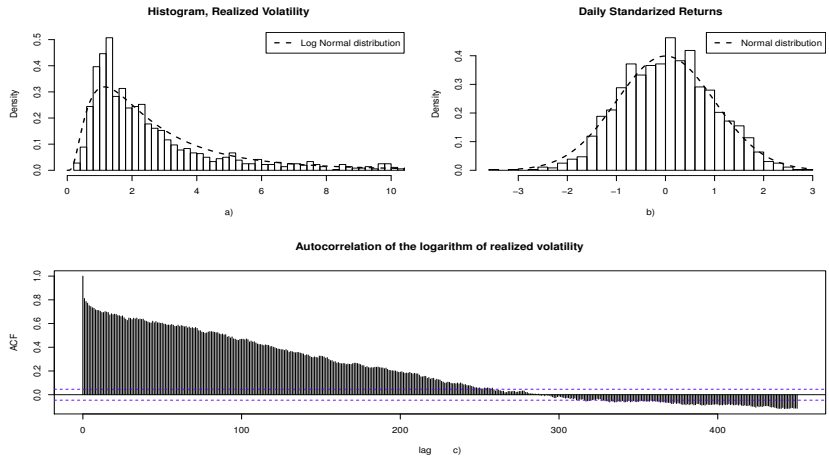

Figure 4.6: *a) The distribution of realized volatility for the ICE Brent Crude Future contracts. b) The distribution of the daily standardized returns for ICE Brent Crude Future contracts. c) Autocorrelations for the logarithm of realized volatility for the ICE Brent Crude Future contracts. All three figure are based on data from 1/1/2005 to 31/1/2012.*

4.3 Realized measures

The realized measures introduced in the quadratic variation theory include realized variance, jump variation, realized bipower variation and continuous variation. These measures are designed to split the volatility into different categories, which is easier to interpret. The jump- and continuous variation are measures related to the realized variance. Figure 4.7 shows realized volatility computed for the total sample period with 3, 5, 10, 15 and 30 minutes returns. The realized volatility is calculated using data from open (01:00, London local time) to close (22:00, London local time) while taking into account the shift from GMT to BST. We also adopted the realized kernel as our realized measure. This estimator is similar to the realized variance, but more robust to differences obtained from bid/ask spread and various noise. The implementation follows a simplified version of the kernel introduced by (Barndorff-Nielsen, Hansen, Lunde & Shephard 2008).

Since the microstructure noise would effect the lowest resolution of data, the realized kernel was only implemented for our 3 minute returns. This gave no significant improvement, indicating that the effect of microstructure noise on our 3 minute returns are quite low. Table 4.2 shows descriptive statistics for the realized variance based on all observation frequencies. The mean, min and max show a clear increase for lower observation frequencies. This suggests that there are more variation included in lower frequencies then for higher. The standard deviation are more similar but does also show the same pattern. The skewness and kurtosis suggest that the data is leptokurtic. The increase for higher frequencies are a result related to the sample sizes. The hypothesis for normality in the Jarque-Bera statistic is rejected at the 1% significance level. The Ljung-Box statistic which tests if

Descriptive Statistics for Realized Volatility											
	Mean	Min	Max	St.Dev.	Kurt	Skew	JB	$Q(10)$	ADF	ρ_1	ρ_{10}
RV_{3min}	3.090	0.253	42.54	3.42	25.02	3.69	40643	6804.4	-4.01	0.711	0.588
RV_{5min}	3.004	0.205	43.02	3.42	26.67	3.86	46587	6489.0	-4.07	0.695	0.577
RV_{10min}	2.929	0.180	41.01	3.37	26.15	3.86	44771	6379.8	-3.82	0.696	0.561
RV_{15min}	2.886	0.186	41.73	3.41	26.53	3.92	46257	5982.2	-3.99	0.668	0.564
RV_{30min}	2.812	0.162	41.72	3.39	27.11	3.95	48375	5397.5	-4.23	0.629	0.530

Table 4.2: *Descriptive statistics for the ICE Brent Crude future contracts with 3,5,10,15 and 30 minute realized variance. The table shows mean, min, max, standard deviation, kurtosis, skewness, JB is the Jarque-Bera statistic to test the null hypothesis of normality, Q(10) is the Ljung-Box statistic adjusted for heteroskedasticity following (Diebold 1988) to test the null hypothesis of no autocorrelations up to 10 lags, ADF is the Augmented Dickey-Fuller test for the null hypothesis that the series have a unit root and ρ_1, ρ_{10} is autocorrelation at lag 1 and 10 respectively.*

the data is independently distributed (no correlation) are also rejected at the 1% significance level. This result is consistent with the well known phenomenon of volatility clustering. This is also shown by ρ_1 and ρ_{10} which shows autocorrelation at lag 1 and 10 respectively. Figure 4.8 shows the auto correlation function for 3, 5, 10, 15 and 30 minute returns. There is high persistence in correlation, indicating that all the samples can be compared to a long memory process. The Augmented Dickey-Fuller test also rejects the null hypothesis that the series have a unit root at the 1% significance level. In the quadratic variation theory section we intro-

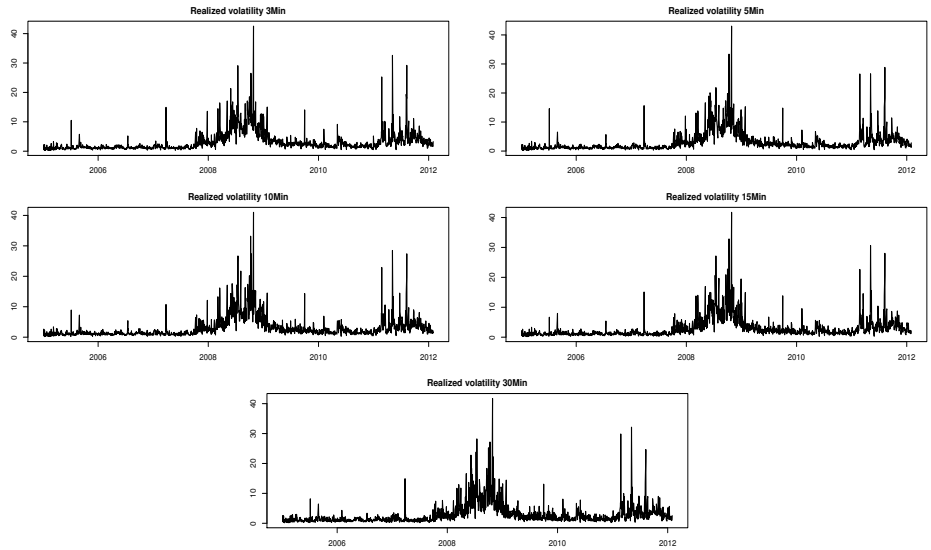

Figure 4.7: *The figure shows realized variance for the ICE Brent Crude Oil futures front month contract with observation frequency 3, 5, 10,15 and 30 minutes respectively. All figures are based on intraday data from 1/1/2005 to 31/1/2012.*

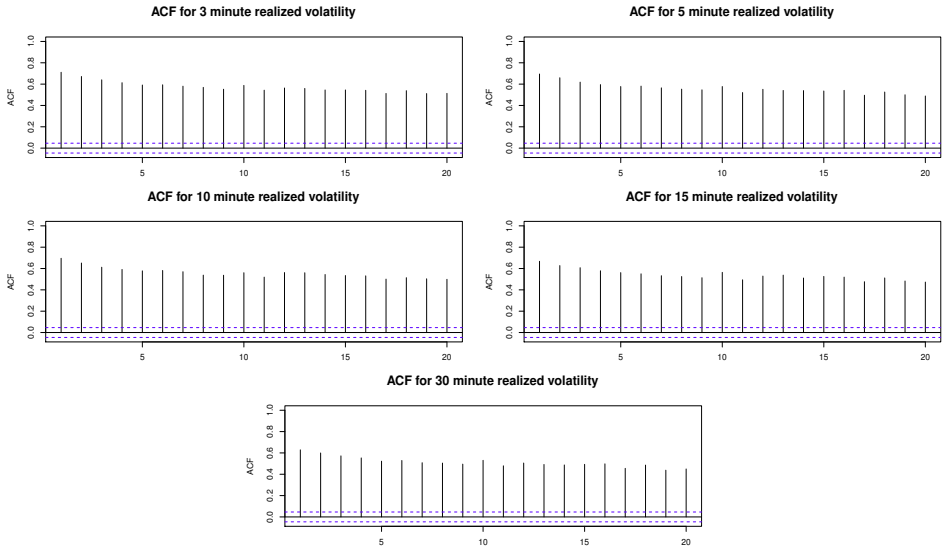

Figure 4.8: *The Figure shows realized variance based on 3, 5, 10, 15 and 30 minute returns. The figures are based on intraday data from 1/1/2005 to 31/1/2012.*

duced the notion of splitting the realized volatility into a continuous and a jump component. Jumps in returns are highly responsible for the asymmetries which is observed in the leverage function. The jumps often represents shocks in return which again effects volatility. (Hamilton 2011) found that events in the oil market are important for policy makers since shocks in price is often followed by economic downturn. Table 4.3 shows descriptive statistics for continuous and jump volatility. Since these measures are components of the realized volatility they exhibit the same properties as we found for the realized volatility. The jump percentage [3] is similar between observation frequencies indicating that the Z-test statistic is biased.

Table 4.4 shows detailed descriptive statistics for jump volatility based on 3 minute intraday returns. The jump percentage is similar across different years, but increased between 2007-2009. Hence, we would assume that the jump volatility would increase in the financial crisis period. This is only an assumption, with not enough significant evidence to back it up. The daily average jump intensity is similar for all years. Figure 4.9 shows continuous volatility and jump volatility for 3 minute and 30 minute returns. The jump volatility is constructed using a indicator function where the value is zero for non jump days and the JV value for jump days.

[3]The jump percentage is calculated by counting the number of days with return jumps and dividing it with the total sample size.

Descriptive Statistics for Continuous Volatility and Jump Volatility							
	Mean	Min	Max	St.Dev.	Kurt	Skew	Jump %
CV_{3min}	2.5609	0.065	24.69	2.76	16.4	3.11	-
JV_{3min}	0.5295	0	30.15	1.25	194	10.5	49 %
CV_{5min}	2.6025	0.059	33.38	2.91	23.8	3.62	-
JV_{5min}	0.4017	0	33.04	1.29	252	12.3	43 %
CV_{10min}	2.5704	0.063	28.48	2.81	19.3	3.31	-
JV_{10min}	0.3591	0	34.41	1.35	251	12.4	39 %
CV_{15min}	2.5372	0.042	32.84	2.87	25.6	3.79	-
JV_{15min}	0.3489	0	32.52	1.38	190	10.8	44 %
CV_{30min}	2.4912	0.049	32.13	3.01	25.9	3.92	-
JV_{30min}	0.3210	0	33.04	1.34	226	11.8	36 %

Table 4.3: *Descriptive statistics for the ICE Brent Crude future contracts with 3,5,10,15 and 30 minute continuous and Jump Volatility. The table shows mean, min, max, standard deviation, kurtosis, skewness and jump percentage based on the intraday Z-test statistic.*

Jump Descriptive Statistics

Year	% Days with Return jumps	N. days with Return Jumps	Average Jump intensity (Day)	Max Jump intensity (Day)
2005	40.40	101	1.49	14
2006	37.11	95	1.92	17
2007	57.97	147	1.82	11
2008	59.13	149	1.72	12
2009	53.15	135	1.59	13
2010	43.57	112	1.47	9
2011	46.24	119	1.42	8
2012*	14.20	3	0.58	2

Table 4.4: *Descriptive statistics for jump volatility based on 3 minute intraday returns. The table shows percentage of days with return jumps, number of days with return jumps, average intensity and maximum jump intensity. The intraday Z-test statistic has been used to estimate the values. * The data only shows the first month of the year.*

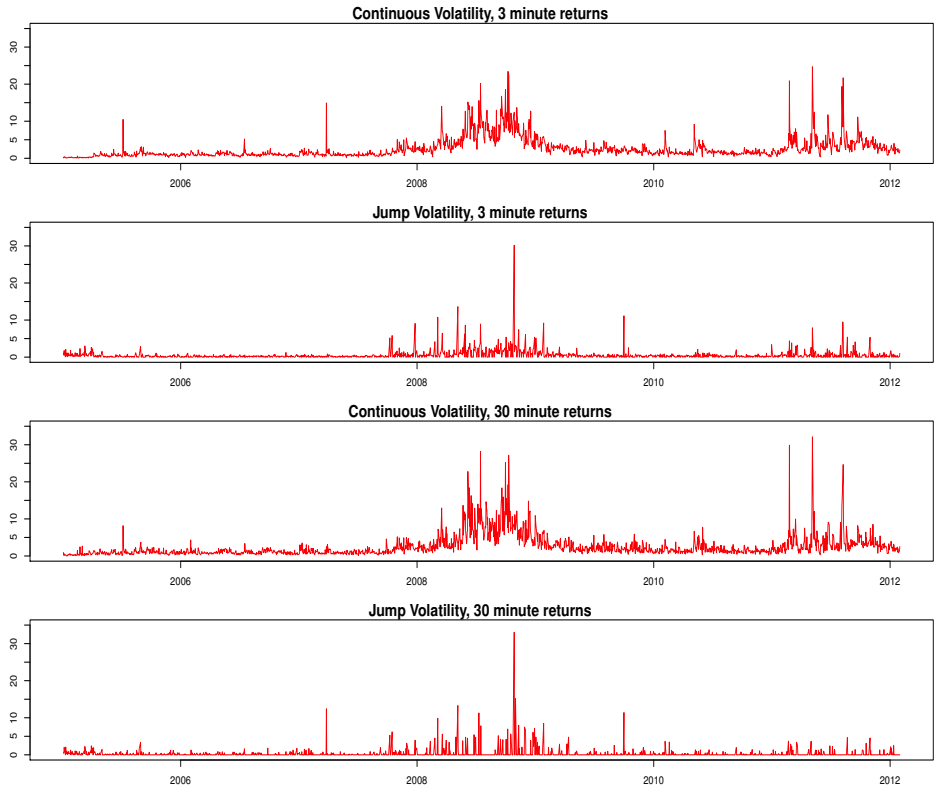

Figure 4.9: *The figure shows 3 and 5 minute continuous and jump volatility. All figures are based on data from 1/1/2005 to 31/1/2012.*

4.4 Empirical Results for the Log-Linear Realized GARCH model

In this section we present results for the Realized GARCH model with a log-linear specification. We use $RG(p,q)$ to denote the log-linear Realized GARCH model with p lags of h_t and q lags of x_t. The model will be estimated with the parameters $p = 1$ and $q = 2$. The model will be estimated for five different observation frequencies and for the sake of comparison we use the logarithmic GARCH(1,1) model. Results will be reported for the total sample and a rolling window for the out of sample comparison. Distributions will be included for the standardized error term z_t in Eq (3.1) and the conditional correlations, ρ^- and ρ^+ will be represented together with the news impact curve.

4.4.1 Log-Linear Realized GARCH for total sample (Table 4.5)

Table 4.5 shows parameter estimates for the log-linear realized GARCH(1,2) model for the total sample series. The empirical results are based on realized volatility included in the measurement equation with observation frequencies 3, 5, 10, 15 and 30 minutes. The robust standard errors (in bracers) together with the t-statistics suggests that all parameters are significant. The estimate of ϕ in the measurement equation is close to one, $\hat{\phi} \simeq 1$, for all observation frequencies, but decreases when the frequency increases. This suggests that the realized measure, x_t, which is in our case the realized volatility, is proportional to the conditional variance for all the observation frequencies. The decrease in this parameter suggests that the lower observation frequencies is a better explanatory measure then higher frequencies. The parameter ξ in the measurement equation is close to zero for all the frequencies, suggesting that the realized measure is computed over a very similar period. The model seems to distinguish between the different frequencies even though the realized measure are calculated based on the same period.

The β parameter in the *GARCH equation* is also given more weight when the observation frequency increases. This suggest that the measurement equation is more significant for lower observation frequencies, giving more weight to the realized measures. This is also consistent with the decrease for the error term in the measurement equation. The parameter σ_u shows a clear increase for increasing observation frequencies. In terms of the log-likelihood function, $l(x,r)$, the 3 minute observation frequencies leads to a much better empirical fit then the 5 minute frequency. The drop from -4118.0 to -4021.1 is quite significant without the need of further statistical testing. The gap between the other frequencies is also significant, leading to a approximately linear improvement in the log-likelihood function. The numerical optimization algorithm resulted in strong convergence for all the observation frequencies.

Total Sample
Point Estimates and Log-Likelihood

Model	$RG_{3\ min}$	$RG_{5\ min}$	$RG_{10\ min}$	$RG_{15\ min}$	$RG_{30\ min}$
ω	-0.01	-0.00	0.00	0.01	0.01
	(0.01)	(0.01)	(0.00)	(0.01)	(0.01)
α					
β	0.82	0.84	0.83	0.85	0.86
	(0.03)	(0.02)	(0.03)	(0.02)	(0.02)
γ_1	0.34	0.34	0.30	0.29	0.24
	(0.03)	(0.03)	(0.03)	(0.03)	(0.03)
γ_2	-0.17	-0.18	-0.13	-0.14	-0.09
	(0.04)	(0.04)	(0.04)	(0.03)	(0.03)
ξ	0.09	0.06	0.03	0.00	-0.04
	(0.04)	(0.04)	(0.04)	(0.04)	(0.04)
ϕ	0.98	0.97	0.97	0.97	0.96
	(0.04)	(0.05)	(0.04)	(0.04)	(0.04)
σ_u	0.39	0.41	0.43	0.45	0.51
	(0.00)	(0.01)	(0.01)	(0.01)	(0.01)
τ_1	-0.04	-0.04	-0.04	-0.05	-0.05
	(0.01)	(0.01)	(0.01)	(0.01)	(0.01)
τ_2	0.05	0.05	0.06	0.06	0.08
	(0.01)	(0.01)	(0.01)	(0.01)	(0.01)
$l(r,x)$	-4021.1	-4118.0	-4215.9	-4314.6	-4516.4
$l(r)$	-3180.6	-3180.9	-3176.9	-3181.5	-3181.6
π	0.993	0.993	0.992	0.993	0.993

Table 4.5: *Results with the log-linear specification for ICE Brent Crude Oil front month contract: RG donates the realized GARCH model with parameters $p = 1$ and $q = 2$. The subscripts donates 3,5,10,15 and 30 minute realized variance. The standard errors (in brackets) are robust standard errors. $l(r,x)$ and $l(r)$ represents the total log-likelihood function and the log-likelihood function for the GARCH equation respectively.*

4.4.2 Log-Linear Realized GARCH for out of sample (Table 4.7)

Table 4.6 shows log-likelihood estimates for the log-linear realized GARCH(1,2) model with a rolling window series. The rolling window is constructed by taking the average over the total amount of simulations. The table show 1000, 1200, 1400 and 1600 observation series for the five different realized measure frequencies. The results are similar to the total sample estimates. All the rolling windows show the same approximately linear increase in the log-likelihood function. This indicates that the 3 minute realized variance is a significantly better estimate then for realized variance constructed from higher observation frequencies. Table 4.7 shows

Out of Sample Log-Likelihood

Window	$RG_{3\ min}$	$RG_{5\ min}$	$RG_{10\ min}$	$RG_{15\ min}$	$RG_{30\ min}$
w = 1000	-2950.4	-3012.4	-3092.5	-3198.2	-3302.6
w = 1200	-3202.1	-3264.6	-3340.4	-3470.5	-3590.2
w = 1400	-3516.5	-3569.8	-3664.5	-3772.4	-3945.1
w = 1600	-3845.1	-3901.2	-3998.2	-4130.1	-4234.2

Table 4.6: *Results for the log-linear realized GARCH(1,2) model for the ICE Brent Crude future front month contract. w donates the sample size for the rolling window estimates. RG donates the realized GARCH(1,2) model with different observation frequencies for the realized measure.*

both the log-likelihood and point estimates for the rolling window with a sample size of 1400. The estimate of ϕ is closer to unity for the out of sample forecasts indicating that the realized measures are given more weight.

All the parameters are exhibiting the same properties we found for the total sample estimates. Taking into account the sample size, the gap between 3 minute and 5 minute realized volatility is still significant, but less then what we found for the total sample. The likelihood estimate for the GARCH equation, $l(r)$, should remain constant, since the realized measures only effects the estimates for the measurement equation. The leverage parameters τ_1 and τ_2 also changes in magnitude for the out of sample forecast, which we will discuss in the preceeding sections.

Out of Sample
Point Estimates and Log-Likelihood

Model	$RG_{3\ min}$	$RG_{5\ min}$	$RG_{10\ min}$	$RG_{15\ min}$	$RG_{30\ min}$
ω	-0.01	0.00	0.00	0.01	0.02
	(0.01)	(0.01)	(0.01)	(0.01)	(0.01)
α					
β	0.83	0.84	0.83	0.85	0.84
	(0.03)	(0.03)	(0.03)	(0.02)	(0.02)
γ_1	0.39	0.38	0.35	0.32	0.25
	(0.03)	(0.03)	(0.03)	(0.03)	(0.03)
γ_2	-0.22	-0.23	-0.19	-0.17	-0.09
	(0.04)	(0.04)	(0.04)	(0.04)	(0.04)
ξ	0.08	0.04	0.01	-0.02	-0.07
	(0.06)	(0.06)	(0.05)	(0.05)	(0.05)
ϕ	0.99	0.99	0.99	0.99	0.98
	(0.05)	(0.05)	(0.05)	(0.05)	(0.05)
σ_u	0.38	0.39	0.42	0.44	0.50
	(0.00)	(0.01)	(0.01)	(0.01)	(0.01)
τ_1	-0.04	-0.04	-0.05	-0.05	-0.05
	(0.01)	(0.01)	(0.01)	(0.01)	(0.01)
τ_2	0.05	0.05	0.06	0.06	0.07
	(0.01)	(0.01)	(0.01)	(0.01)	(0.01)
$l(r,x)$	-3516.5	-3569.8	-3664.5	-3772.4	-3945.1
$l(r)$	-2830.2	-2829.7	-2825.2	-2830.2	-2830.2
π	0.993	0.993	0.992	0.993	0.993

Table 4.7: *Results with the log-linear specification for ICE Brent Crude Oil front month contract: RG donates the realized GARCH model with parameters $p = 1$ and $q = 2$. The subscripts donates 3,5,10,15 and 30 minute realized variance. The standard errors (in brackets) are robust standard errors. $l(r, x)$ and $l(r)$ represents the total log-likelihood function and the log-likelihood function for the GARCH equation respectively. The results are based on a rolling window with $w = 1400$ observations.*

4.4.3 Log-Linear Realized GARCH model with distributions related to the standard GARCH model (Table 4.8)

Table 4.8 shows the Log-linear realized GARCH(1,2) model based on 3 minute realized volatility. The table also includes results for the logarithmic GARCH(1,1) model and the realized GARCH model with the normal, student's t and skewed student's t distribution. The log-likelihood function, $l(r)$, clearly shows a significant improvement compared to the LGARCH(1,1) model. Technically, the logarithmic GARCH(1,1) model leads to a worse fit then the GARCH(1,1) model, but the difference is not significant in this context. Judging from the estimated values of the log-likelihood, the skewed student's t distribution leads to the best fit. The log-likelihood ratio statistic only gave weak evidence for the inclusion of the skewed student's t distribution.

The skew parameter, ϵ, suggests that the standardized error term, z_t, has a negative skewness. Although, the degree of freedom for the student's t distributed indicates a strong resemblance to the normal distribution, but with heavier tails. Figure 4.10 shows the different distributions with their respective estimated values. The persistence in volatility, which can be measured by the estimate $\beta + \gamma\phi$, is close to 0.99 for each distribution. This shows that there is a high persistence in volatility which is common in many financial markets.

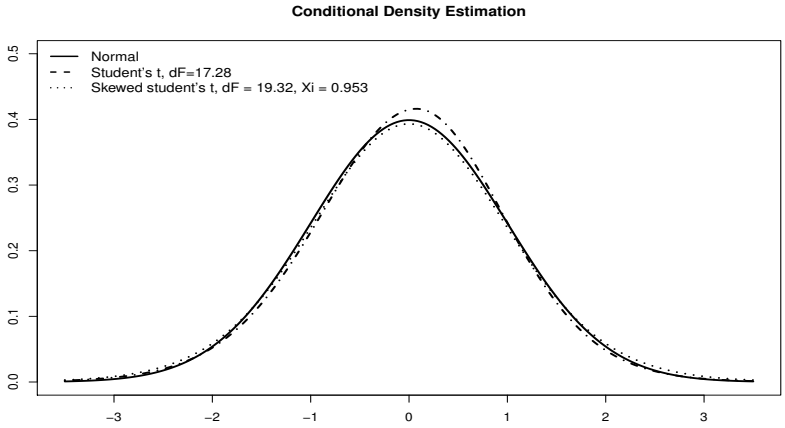

Figure 4.10: *The figure shows estimated values for the normal, student's t and skewed student's t distributions. The distributions are fitted to the standardized error term, z_t, in the return equation.*

Total Sample
Point Estimates and Log-Likelihood

Model	$LG(1,1)$	RG_{Normal}	$RG_{Student's\ t}$	$RG_{Skewd\ Stud\ t}$
ω	0.03	-0.01	-0.03	-0.02
	(0.00)	(0.01)	(0.01)	(0.01)
α	0.04			
	(0.00)			
β	0.92	0.82	0.83	0.81
	(0.00)	(0.03)	(0.03)	(0.03)
γ_1		0.34	0.34	0.35
		(0.03)	(0.03)	(0.03)
γ_2		-0.17	-0.17	-0.18
		(0.04)	(0.04)	(0.04)
ξ		0.09	0.20	0.17
		(0.04)	(0.05)	(0.04)
ϕ		0.98	1.01	1.00
		(0.04)	(0.05)	(0.04)
σ_u		0.39	0.39	0.38
		(0.00)	(0.01)	(0.01)
τ_1		-0.04	-0.04	-0.04
		(0.01)	(0.01)	(0.01)
τ_2		0.05	0.05	0.06
		(0.01)	(0.01)	(0.01)
ν	-	-	17.28	19.32
			(3.71)	(4.21)
ϵ	-	-	-	0.953
				(0.09)
$l(r,x)$	-	-4021.1	-4012.2	-4001.9
$l(r)$	-3293.5	-3180.6	-3168.6	-3159.9
π	0.995	0.993	0.993	0.992

Table 4.8: *Results with the log-linear specification for ICE Brent Crude Oil front month contract: RG donates the realized GARCH model with parameters $p = 1$ and $q = 2$. LG(p,q) donates the logarithmic GARCH model with parameters $p = 1$ and $q = 1$. The subscripts donates the normal, student's t and skewed student's t distributions. The standard errors (in brackets) are robust standard errors. $l(r,x)$ and $l(r)$ represents the total log-likelihood function and the log-likelihood function for the GARCH equation respectively. The results are based on a rolling window with $w = 1400$ observations.*

4.5 News impact curve

The inclusion of high frequency data enable us to make a more detailed prediction about the news impact curve then for daily/weekly returns. We have estimated the log-linear realized GARCH(1,2) model based on the hermite polynomial. This polynomial, also called the leverage function, estimates the asymmetry in volatility caused by a shock in the price. Table 4.9 shows both total sample and out of sample estimation of negative and positive asymmetry between return and volatility. The asymmetry is negatively weighted for all the frequencies of realized volatility. Out of sample estimation emphasizes this result, showing that there is a clear negative correlation between price shocks and volatility. Figure 4.11 gives a visual

Total Sample Correlation					
Window	$RG_{3\ min}$	$RG_{5\ min}$	$RG_{10\ min}$	$RG_{15\ min}$	$RG_{30\ min}$
ρ^-	-0.136	-0.139	-0.118	-0.176	-0.216
ρ^+	0.108	0.107	0.091	0.133	0.172
Out of Sample Correlation					
Window	$RG_{3\ min}$	$RG_{5\ min}$	$RG_{10\ min}$	$RG_{15\ min}$	$RG_{30\ min}$
ρ^-	-0.150	-0.148	-0.159	-0.188	-0.231
ρ^+	0.091	0.087	0.101	0.118	0.152

Table 4.9: *Results for the log-linear realized GARCH(1,2) leverage function. ρ^- and ρ^+ are negative and positive asymmetry respectively. RG donates the realized GARCH model with subscript related to the observation frequency. The out of sample estimation is based on a rolling window with $w = 1400$ observations.*

representation of the result. The news impact curve is calculated based on 3, 5, 10 ,15 and 30 minute realized volatility, where the horizontal axis is z_{t-1} and the vertical axis is σ_t. Even though the estimates in Table 4.9 are greater in magnitude for higher observation frequencies they represent the same effect. Figure 4.11 shows small differences in the estimated news impact curve for the different frequencies. The result are as expected, since the estimates for different observation frequencies should indicate the same asymmetries. Figure 4.12 shows the 3 minute estimated asymmetry together with the news impact curve for Chevron Corporation and Exxon Mobil Corporation, two of the biggest oil companies in the world. The stock spot price for the two oil companies shows the same asymmetry, but they differ in magnitude.

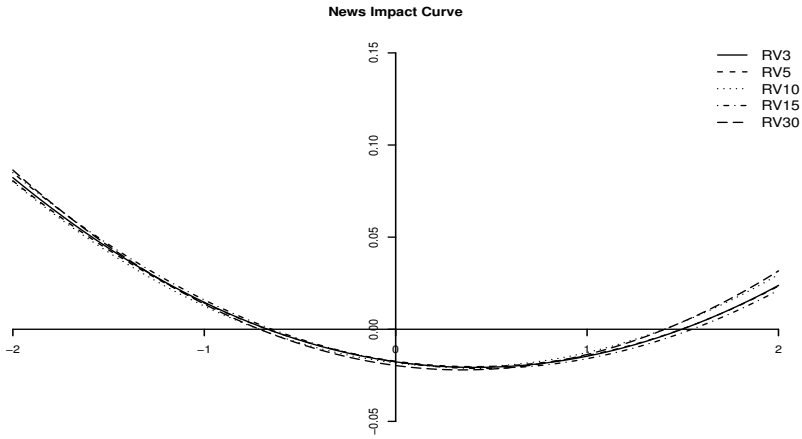

Figure 4.11: *The figure shows the news impact curve based on the log-linear realized GARCH estimates. The curves are based on 3,5,10,15 and 30 minute realized measures. The horizontal axis is z_{t-1} and the vertical axis is σ_t.*

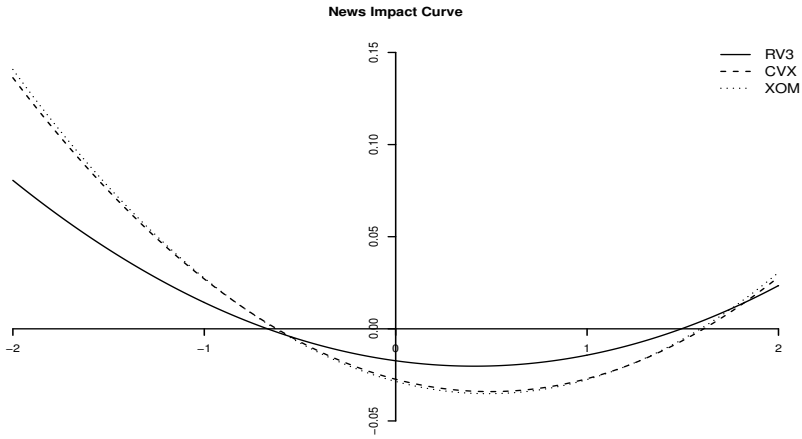

Figure 4.12: *The figure shows the news impact curve based on the log-linear realized GARCH estimates. The curves are based on 3 minute realized measure, Chevron Corporation and Exxon Mobil Corporation (Hansen at.all. 2011). The horizontal axis is z_{t-1} and the vertical axis is σ_t.*

Chapter 5

Conclusion

In this paper we described and suggested the use of a realized GARCH model to analyze the ICE Brent Crude oil front month contracts using high frequency data to construct realized measures. This is the first paper, as far as we know, that uses the realized GARCH model to analyze the forward ICE Brent Crude oil future market. The descriptive statistics suggest a positive skewness and kurtosis greater then three for the realized volatility. Moreover, as for realized volatility, continuous and jump volatility show similar skewness and kurtosis characteristics. The classical and the realized GARCH model, seem to be well specified and show strong convergence for all estimations. The realized GARCH model shows an improved log-likelihood relative to the standard GARCH model. The results suggests that use of high frequency data improve the modeling of conditional volatility. The realized measures might therefore incorporate more relevant information. The results also give weak evidence for the skewed student's t distribution in the standardized error term, z_t.

There is a clear negative asymmetry between return and conditional volatility. The results are also similar across different observation frequencies. The residuals show low, to no data dependence, and indicate that the model are appropriate for the data series. Finally, the significance of the realized GARCH coefficients clearly indicate a need for more information in the conditional volatility. For future research it will be interesting to look at model assessment, and to test model residuals. Tests for the optimal amount of latent volatility factors for different models, (MEM), (HEAVY) and Realized GARCH. Predictions of future volatility of realized versus classical GARCH using forecast evaluation statistics. Extensions to multivariate GARCH models, extreme value theory, risk management (VaR/CVaR) and asset allocation measures (Greek letters).

Chapter 6

Bibliography

Andersen, T. & Bollerslev, T. (1998), 'Answering the skeptics: Yes, standard volatility models do provide accurate forecasts', *International Economic Review* pp. 885–905.

Andersen, T., Bollerslev, T. & Diebold, F. (2007), 'Roughing it up: Including jump components in the measurement, modeling, and forecasting of return volatility', *The Review of Economics and Statistics* **89**(4), 701–720.

Andersen, T., Bollerslev, T., Diebold, F. & Ebens, H. (2001), 'The distribution of realized stock return volatility* 1', *Journal of Financial Economics* **61**(1), 43–76.

Andersen, T., Bollerslev, T. & Dobrev, D. (2007b), 'No-arbitrage semi-martingale restrictions for continuous-time volatility models subject to leverage effect, jumps and iid noise: Theory and testable distributional implications.', *Journal of Econometrics* **138**, 125–180.

Andersen, T., Bollerslev, T., Fredriksen, P. & Ørregaard Nielsen, M. (2010), 'Continuous-time models, realized volatilities, and testable distributional implications for daily stock returns.', *Journal of Applied Econometrics* **25**, 233–261.

Athreya, K. & Pantula, S. (1986), 'A note on strong mixing of arma processes', *Statistics probability letters* **4**(4), 187–190.

Barndorff-Nielsen, O., Hansen, P., Lunde, A. & Shephard, N. (2008), 'Designing realized kernels to measure the ex post variation of equity prices in the presence of noise', *Econometrica* **76**(6), 1481–1536.

Barndorff-Nielsen, O. & Shephard, N. (2001), 'Non-gaussian ornstein-uhlenbeck-based models and some of their uses in financial economics', *Journal of the Royal Statistical Society: Series B (Statistical Methodology))* **63**(2), 167–241.

Barndorff-Nielsen, O. & Shephard, N. (2004), 'Power and bipower variation with stochastic volatility and jumps', *Journal of financial econometrics* **2**(1), 1.

Bollerselv, T. (1986), 'Generalized autoregressive conditional heteroskedasticity', *Journal of Econometrics* **31**(3), 307–327.

Bollerslev, T. (2009), 'Glossary to arch (garch)', *Oxford University Press, Oxford, UK* .

Bollerslev, T., Kretschmer, U., Pigorsch, C. & Tauchen, G. (2009), 'A discrete-time model for daily s & p500 returns and realized variations: Jumps and leverage effects', *Journal of Econometrics* **150**(2), 151–166.

Bystrom, H. (2005), 'Extreme value theory and extremely large electricity price changes', *International Review of Economics & Finance* **14**(1), 41–55.

Carrasco, M. & Chen, X. (2002), 'Mixing and moment properties of various garch and stochastic volatility models', *Econometric Theory* **18**(1), 17–39.

Chen, X. & Ghysels, E. (2010), 'News-good or bad-and its impact on predicting future volatility', *Review of Financial Studies* .

Chen, X., Ghysels, E. & Wang, F. (2009), The class of hybrid-garch models, Technical report, Discussion Paper UNC.

Comte, F. & Renault, E. (1998), 'Long memory in continuous-time stochastic volatility models', *Mathematical Finance* **8**(4), 291–323.

Dacorogna, M. (2001), 'An introduction to high-frequency finance', *Academic Paper* .

Diebold, F. X. (1988), *Empirical modeling of exchange rate dynamics.*, Lecture Notes in Economics and Mathematical Systems, 303. Berlin etc.: Springer-Verlag. 143 p. DM 32.00 .

Engle, R. (1982), 'Autoregressive conditional heteroscedasticity with estimates of the variance of united kindom inflation', *Econometrica: Journal of the Econometric Society* pp. 987–1007.

Engle, R. & Gallo, G. (2006), 'A multiple indicators model for volatility using intradaily data', *Journal of Applied Econometrics* **131**(1-2), 3–27.

Engle, R. & Ng, V. (1991), Measuring and testing the impact of news on volatility, Technical report, National Bureau of Economic Research.

Fernández, C. & Steel, M. (1998), 'On bayesian modeling of fat tails and skewness', *Journal of the American Statistical Association* pp. 359–371.

Geweke, J. (1986), 'Exact inference in the inequality constrained normal linear regression model', *Journal of Applied Econometrics* **1**(2), 127–141.

Hamilton, J. (2011), Historical oil shocks, Technical report, National Bureau of Economic Research.

Hansen, B. (1994), 'Autoregressive conditional density estimation', *International Economic Review* pp. 705–730.

Hansen, P., Huang, Z. & Shek, H. (2011), 'Realized garch: A complete model of returns and realized measures of volatility', *Journal of Applied Econometrics. forthcoming* .

Huang, X. & Tauchen, G. (2005), 'The relative contribution of jumps to total price variance', *Journal of Financial Econometrics* **3**(4), 456.

Lambert, P. & Laurent, S. (2000), 'Modelling skewness dynamics in series of financial data', *Institut de Statistique* .

Lambert, P. & Laurent, S. (2002), 'Modelling skewness dynamics in series of financial data using skewed location-scale distributions', *Institut de Statistique, Louvain-la-Neuve Discussion Paper* **119**.

Lee, S. & Mykland, P. (2008), 'Jumps in financial markets: A new nonparametric test and jump dynamics.', *Review of Financial Studies* **21**, 2535–2563.

Nelson, D. (1991), 'Conditional heteroskedasticity in asset returns: A new approach', *Econometrica* **59**, 347–370.

Shephard, N. & Sheppard, K. (2010), 'Realising the future: forcasting with high frequency-based volatility (heavy) models', *Journal of Applied Econometrics* **25**(2), 197–231.

Taylor, S. (2007), *Asset price dynamics, volatility, and prediction*, Princeton Univ Pr.